Available online at www.sciencedirect.com

ScienceDirect

Geochimica et Cosmochimica Acta 181 (2016) 18–35

Geochimica et Cosmochimica Acta

www.elsevier.com/locate/gca

Stable carbon isotope ratios of intact GDGTs indicate heterogeneous sources to marine sediments

Ann Pearson [a,*], Sarah J. Hurley [a], Sunita R. Shah Walter [a], Stephanie Kusch [a,1], Samantha Lichtin [b], Yi Ge Zhang [a]

[a] Department of Earth and Planetary Sciences, Harvard University, Cambridge, MA 02138, USA
[b] Department of Geology and Geophysics, Yale University, New Haven, CT 06520, USA

Received 9 December 2015; accepted in revised form 29 February 2016; Available online 3 March 2016

Abstract

Thaumarchaeota, the major sources of marine glycerol dibiphytanyl glycerol tetraether lipids (GDGTs), are believed to fix the majority of their carbon directly from dissolved inorganic carbon (DIC). The $\delta^{13}C$ values of GDGTs ($\delta^{13}C_{GDGT}$) may be powerful tools for reconstructing variations in the ocean carbon cycle, including paleoproductivity and water mass circulation, if they can be related to values of $\delta^{13}C_{DIC}$. To date, isotope measurements primarily are made on the C_{40} biphytane skeletons of GDGTs, rather than on complete tetraether structures. This approach erases information revealed by the isotopic heterogeneity of GDGTs within a sample and may impart an isotopic fractionation associated with the ether cleavage. To circumvent these issues, we present $\delta^{13}C$ values for GDGTs from twelve recent sediments representing ten continental margin locations. Samples are purified by orthogonal dimensions of HPLC, followed by measurement of $\delta^{13}C$ values by Spooling Wire Microcombustion (SWiM)-isotope ratio mass spectrometry (IRMS) with 1σ precision and accuracy of $\pm 0.25‰$. Using this approach, we confirm that GDGTs, generally around $-19‰$, are isotopically "heavy" compared to other marine lipids. However, measured $\delta^{13}C_{GDGT}$ values are inconsistent with predicted values based on the ^{13}C content of DIC in the overlying water column and the previously-published biosynthetic isotope fractionation for a pure culture of an autotrophic marine thaumarchaeon. In some sediments, the isotopic composition of individual GDGTs differs, indicating multiple source inputs. The data appear to confirm that crenarchaeol primarily is a biomarker for Thaumarchaeota, but its $\delta^{13}C$ values still cannot be explained solely by autotrophic carbon fixation. Overall the complexity of the results suggests that both organic carbon assimilation (*ca.* 25% of total carbon) and multiple source(s) of exogenous GDGTs (contributing generally <30% of input to sediments) are necessary to explain the observed $\delta^{13}C_{GDGT}$ values. The results suggest caution when interpreting the total inputs of GDGTs to sedimentary records. Biogenic or open-slope sediments, rather than clastic basinal or shallow shelf sediments, are preferred locations for generating minimally-biased GDGT proxy records.

1. INTRODUCTION

Archaeal GDGTs are ubiquitous in marine sediments and form the basis of the sea surface temperature (SST) proxy known as TEX_{86} (Schouten et al., 2002). TEX_{86} has been used for paleoclimate reconstructions in both marine and large lacustrine environments, and over timescales from the Jurassic to the present (*e.g.*, Bijl et al., 2010;

* Corresponding author.
E-mail address: pearson@eps.harvard.edu (A. Pearson).
[1] Present address: Institute of Geology & Mineralogy, University of Cologne, 50674 Cologne, Germany.

http://dx.doi.org/10.1016/j.gca.2016.02.034
0016-7037/

Tierney et al., 2010; Jenkyns et al., 2012). The broad geographic and temporal range of GDGTs suggests they will continue to play an important role in interpreting paleotemperatures, even as the scientific community continues to study and debate the mechanistic control(s) on how TEX_{86} works (Elling et al., 2014, 2015; Qin et al., 2015). Although modern TEX_{86} calibrations generally predict SSTs to within ±3–5 °C (Liu et al., 2009; Kim et al., 2010; Tierney and Tingley, 2014), ancient records of TEX_{86}-predicted SSTs can disagree with other proxies and climate models, particularly during greenhouse climates (*e.g.*, Jenkyns et al., 2004; Hollis et al., 2012; Lopes dos Santos et al., 2013). Therefore it is critical to develop a better understanding of the mechanisms controlling GDGT production, export, and deposition (Pearson and Ingalls, 2013).

In most studies to date, the majority of archaeal GDGTs reaching marine sediments are believed to be sourced from planktonic, ammonia-oxidizing Thaumarchaeota, although there is some debate regarding possible additional sources (*e.g.*, Lincoln et al., 2014). Cell numbers and maximum copies of archaeal ammonia monooxygenase (*amoA*) and 16S rRNA genes occur at or just below the base of the photic zone, coincident with nitrification (Massana et al., 1997; Karner et al., 2001; Francis et al., 2005; Church et al., 2010; Santoro et al., 2010). Lipid abundances follow patterns similar to gene copy numbers and cell counts (Schouten et al., 2012; Basse et al., 2014; Lincoln et al., 2014; Xie et al., 2014; Kim et al., 2016). Together these studies suggest that the majority of planktonic thaumarchaeal production is between 100 and 350 m, *i.e.*, dominantly sub-photic. Sub-photic export of GDGTs is consistent with the ratio of GDGT-2 to GDGT-3 ([2/3]) observed in marine sediments. In suspended particulate matter (SPM), [2/3] increases as a function of water column depth, and sedimentary [2/3] values agree better with SPM below the photic zone (Turich et al., 2007; Taylor et al., 2013; Hernandez-Sanchez et al., 2014). Similarly, natural ^{14}C data show that GDGTs recovered from sediments can have older "ages" than co-occurring phytoplanktonic lipids such as sterols (Pearson et al., 2001; Shah et al., 2008). Sub-photic water column export, however, cannot be easily distinguished from the confounding effects of erosional GDGT sources, or from inputs from benthic communities. Deep-water and sedimentary production, as well as exogenous inputs, both contribute "old" ^{14}C, especially if the latter is due to the weathering of ancient sedimentary rocks.

Carbon assimilation in the ammonia-oxidizing Thaumarchaeota is believed to be dominantly, though not exclusively, autotrophic (Ouverney and Fuhrman, 2000; Könneke et al., 2005; Qin et al., 2014; Santoro et al., 2015). Although mixotrophy is observed in some strains, it apparently does not contribute the majority of lipid carbon (Wuchter et al., 2003), and the limited available evidence suggests the overall community assimilates *ca.* 80% of its lipid carbon directly from DIC (Ingalls et al., 2006). If these assessments are correct, the ^{13}C content of GDGTs should generally reflect patterns of ^{13}C in water column DIC. In support of this idea, $\delta^{13}C$ values of archaeal biphytanes (C_{40} isoprenoid sidechains of GDGTs) are relatively constant across ocean basins and depositional environments, *ca.* −21‰ (*c.f.*, Schouten et al., 2013). However, the assumption of a dominantly planktonic origin for sedimentary GDGTs has not been rigorously tested, and other studies indicate that non-planktonic sources of GDGTs may be important. In some sediments, biphytanes and GDGTs are observed with values *ca.* −25‰ (Smittenberg et al., 2005; Biddle et al., 2006), significantly outside the range of values observed for SPM (Hoefs et al., 1997). Although in these cases the anomalies were attributed to ^{13}C–depletion within the local DIC pool or to *in-situ* heterotrophy mediated by Archaea growing within the sediments, alternative explanations are possible. These include mixotrophy or heterotrophy among planktonic Thaumarchaeota and contributions from heterotrophic Euryarchaeota (Iverson et al., 2012; Lincoln et al., 2014; Qin et al., 2014). More information is needed about how many sources and processes contribute GDGTs to sediments.

Conversely, if GDGTs in sediments are derived predominantly from autotrophic, planktonic export, they may serve as a paleo-$\delta^{13}C_{DIC}$ proxy (Hoefs et al., 1997; Schouten et al., 1998). Archaeal biphytanes have been used to infer the ^{13}C content of dissolved inorganic carbon (DIC) during Cretaceous ocean anoxic events (Kuypers et al., 2001), previously a challenge due to the absence of carbonate sedimentation in many sections. This concept could be applied to other intervals of Earth history in which carbonates are absent or have been affected by diagenetic processes. Importantly, the use of $\delta^{13}C_{GDGT}$ values to reconstruct DIC is an idea that can be tested in the modern ocean. DIC is depleted in ^{13}C in the Pacific Ocean relative to the Atlantic Ocean at depths below 100 m (Kroopnick, 1985). This represents an unexplored opportunity to validate the paleo-$\delta^{13}C_{DIC}$ proxy, as sub-photic growth of modern Thaumarchaeota would be expected to incorporate this inter-basinal signal.

To test this idea, we examined the ^{13}C content of individual GDGTs extracted from five samples of Atlantic Ocean sediments and six samples of Pacific Ocean sediments to (*i*) test the idea that sedimentary $\delta^{13}C_{GDGT}$ values reflect local water-column profiles of $\delta^{13}C_{DIC}$ and (*ii*) evaluate whether exogenous and mixotrophic (or heterotrophic) inputs of GDGTs are likely to complicate these records. The choice of analytical approach is critical: inter-basinal differences in $\delta^{13}C_{DIC}$ are on the order of 1‰ and many geologic carbon isotope excursions of interest are <2‰ (*e.g.*, ETM-2; Lourens et al., 2005). Here we use a novel method with analytical precision and accuracy ±0.25‰, a resolution that can distinguish minor differences between GDGT sources. Such a method opens a new window of opportunity to test the hypotheses described above.

2. MATERIALS AND METHODS

2.1. Samples

Total lipid extracts (TLEs) were obtained from 12 horizons spanning 10 locations, all from archival samples (stored at −20 °C since collection or extraction; North Atlantic samples at −40 °C) (Table 1). The Santa Monica

Table 1
Station information, GDGT ratios, and $\delta^{13}C_{GDGT}$ values for all samples.

	N. Atl. 4	N. Atl. 11	N. Atl. 18	Carolina	Cariaco	SMB 2	SMB 8	SBB	WA-3	WA-4	WA-7
Sample											
Sample ID	AT 16-1 MC 11	AT 16-1 MC 41	AT 16-1 MC 81	R/V SewardJ BC1	R/V H. Ginez, MC1	Pulse-32	Pulse-32	OXMZ-MV-01	WA9308 A-3	WA9308 A-4(BC)	WA9308 A-7
Latitude	43°21′N	39°52′N	37°26′N	35°50′N	10°31′N	33°44′N	33°44′N	34°14′N	46°35′N	46°45′N	46°45′N
Longitude	60°08′W	69°56′W	74°20′W	74°50′W	64°39′W	118°50′W	118°50′W	120°05′W	124°25′W	125°00′W	126°00′W
Water depth	1080 m	1150 m	1055 m	630 m	1400 m	905 m	905 m	600 m	91 m	690 m	2589 m
Horizon	2–3 cm	0–1 cm	0–1 cm	0–30 cm	13.5–14 cm	1.5–2.5 cm	7.5–8.5 cm	5.5–6.0 cm	grab	0–2 cm	grab
Age (yr)	0–200	0–100	0–100	0–300	< 100	< 50	150–200	< 50	0–100	0–100	300–1000
SST (°C)[a]	8.7	13.9	15.6	20.8	26.0	15.6	15.6	14.4	12.1	12.3	12.3
GDGT ratios											
TEX_{86}^{H}-SST[b]	16.0	18.2	16.9	20.0	26.0	19.3	19.3	15.0	18.6	17.7	15.7
TEX_{86}^{L}-SST[b]	13.1	16.5	14.1	13.8	23.6	20.7	21.0	12.0	14.1	13.9	15.0
Ring Index	2.07	2.22	2.37	2.86	2.80	2.25	2.17	2.33	2.27	2.08	2.11
[2/3]	5.01	4.82	4.92	2.50	3.21	6.90	8.20	23.65	2.24	2.47	4.61
[2/(1+2)]	0.34	0.38	0.35	0.37	0.52	0.44	0.43	0.38	0.38	0.37	0.36
[0/(0+Cr)]	0.58	0.55	0.51	0.40	0.39	0.52	0.54	0.51	0.53	0.58	0.56
BIT Index	0.15	0.13	0.14	0.09	*n/a*	*n/a*	0.16	*n/a*	0.12	0.15	0.11
$\delta^{13}C$ (‰)											
GDGT-0	−19.5 ± 0.1	−19.4 ± 0.1	−19.5 ± 0.1	−19.3 ± 0.2 −19.5 ± 0.1 −19.1 ± 0.1 −19.5 ± 0.0	−19.1 ± 0.2	−18.9 ± 0.1	−18.5 ± 0.4	−19.3 ± 0.1[c] −19.3 ± 0.2[d]	−21.2 ± 0.2	−21.1 ± 0.2	−19.5 ± 0.0
GDGT-1	*n/a*	*n/a*	*n/a*	−20.5 ± 0.1 −20.2 ± 0.2	*n/a*	−19.0 ± 0.2	−18.3 ± 0.3	−19.2 ± 0.4[c]	−23.6 ± 0.1	−22.8 ± 0.1	−19.4 ± 0.0
GDGT-2	−20.1 ± 0.2	−19.2 ± 0.1	*n/a*	−20.3 ± 0.2	*n/a*	−19.2 ± 0.2	−18.4 ± 0.1 −18.6 ± 0.4	−19.1 ± 0.2[c]	−23.7 ± 0.2	−22.9 ± 0.1	−19.3 ± 0.1
Crenarchaeol	−19.6 ± 0.1	−18.9 ± 0.2	−18.8 ± 0.1	−18.7 ± 0.1 −18.7 ± 0.3 −18.8 ± 0.5 −18.6 ± 0.4 −18.8 ± 0.4 −18.8 ± 0.0 −18.7 ± 0.1 −19.1 ± 0.1 −18.9 ± 0.3 −18.8 ± 0.1	−18.7 ± 0.1	−18.8 ± 0.3	−18.5 ± 0.2	−18.9 ± 0.1[c] −18.9 ± 0.2[d]	−20.5 ± 0.1	−20.6 ± 0.1	−19.7 ± 0.2

n/a indicates values that were not measured or did not meet quality control criteria. Multiple $\delta^{13}C_{GDGT}$ values in a single category represent a variety of types of analytical replicates, as explained in the text.

[a] World Ocean Atlas (https://www.nodc.noaa.gov/OC5/woa13/woa13data.html).
[b] Kim et al. (2010)
[c] 5.5–6.0 cm sediment.
[d] 6.0–6.5 cm sediment.

Basin (SMB) and Santa Barbara Basin (SBB) cores were described in Pearson et al. (2001) and Shah et al. (2008). The Cariaco Basin multicore was collected in 2004 and TLE was donated by K. Hughen. The Carolina Margin box core was collected off coastal North Carolina in July, 1996; it was stored frozen until 2011, when it was homogenized (~0–30 cm total depth). North Atlantic (N. Atl.) multicores were collected in September, 2010. The Washington (WA) margin transect was collected in 1993 and donated by F. Prahl.

2.2. Extraction and processing

SMB and SBB TLEs were extracted by Soxhlet distillation as described previously (Pearson et al., 2001), and the Cariaco TLE was prepared using similar methods. TLEs from N. Atl. and WA sediments were prepared by modified Bligh–Dyer extraction on wet sediments (Saenz et al., 2011). The Carolina core material was dried (60 °C), homogenized, and extracted by microwave-assisted solvent extraction, first in 1:1 CH_2Cl_2:CH_3OH (70 °C), then in 9:1 CH_2Cl_2:CH_3OH (100 °C), followed by rinsing and centrifugation of the extracted sediment. Future studies will use consistent extraction methods and will compare intact vs. hydrolyzed (core) GDGTs.

TLEs were separated over SiO_2 (130–270 mesh) into three fractions: less-polar compounds (100% hexane, followed by 25% ethyl acetate:hexane), GDGT core lipids (1:1 ethyl acetate:hexane), and polar compounds (100% ethyl acetate, followed by 100% methanol).

2.3. HPLC methods

Our approach to identification and isolation of pure GDGTs uses the same columns and solvent gradients as earlier work (Ingalls et al., 2006; Shah and Pearson, 2007; Shah et al., 2008). Each GDGT mixture first is separated by normal phase (NP) high-performance liquid chromatography (HPLC) (Fig. 1A). Then the individual GDGTs are purified by reverse phase (RP) HPLC to remove non-GDGT material (Fig. 1B). Compound-specific collection windows for NP-HPLC are defined by screening a preliminary sample by atmospheric pressure chemical ionization-mass spectrometry (APCI-MS) using standard methods (*e.g.*, Hopmans et al., 2000). All targeted GDGTs (GDGT-0 through crenarchaeol) elute in a narrow window of RP-HPLC and are collected in 3 × 1-min time slices: the preceding minute (F1), the GDGT fraction (F2), and the tailing minute (F3) (Fig. 1B, inset).

Prior to each stage of chromatographic purification, GDGT concentrations are estimated by flow injection analysis (FIA) relative to a dilution series of synthetic standard (C_{46}-GTGT) (Huguet et al., 2006). Because these are not co-injections, differences in ion suppression between samples make the results semi-quantitative. The estimated concentrations are used to limit all purifications to a maximum of *ca.* 20 μg total GDGT injection^{-1}; this is less material than used for prior radiocarbon work, which minimizes the risk of column overloading and improves separations

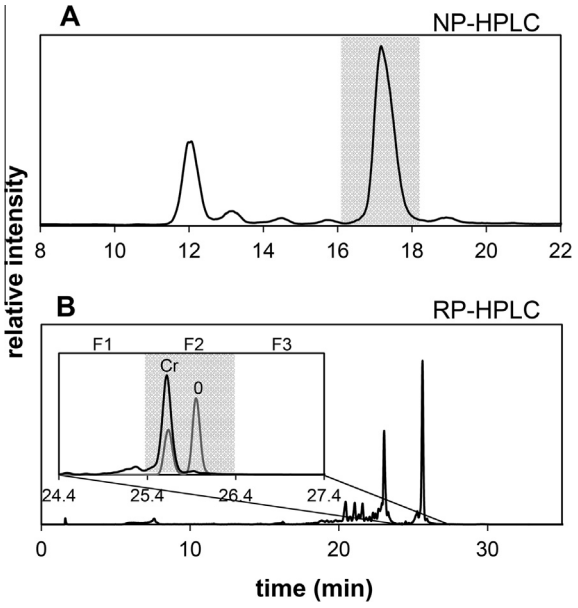

Fig. 1. GDGT fractions are purified by NP-HPLC with fraction collection of each compound (A; crenarchaeol, grey box). The individual compounds – here showing the run for crenarchaeol – are then purified by RP-HPLC to separate non-GDGT material (before 25 min) from GDGTs (B, black trace; and inset, black trace). The purified GDGTs are collected in F2. Re-injection of a mixture of purified crenarchaeol and GDGT-0 demonstrates that the F2 fractions contain no other detectable peaks (*m*/*z* 300–1350) and that the full range of GDGT polarity elutes within the F2 window (B, inset, grey trace).

(Ingalls et al., 2006; Shah and Pearson, 2007; Shah et al., 2008).

Purified GDGT fractions are dried under N_2 and stored in a laminar flow hood. Immediately prior to isotopic analysis, fractions are dissolved in 25 μl ethyl acetate. After IRMS, the remaining material is re-analyzed by FIA and quantified relative to C_{46}-GTGT. The RP-HPLC, IRMS, and final FIA steps always are performed on the same day. APCI-MS mass scanning from *m*/*z* 300–1350 for FIA maximizes detection of all ionizable compounds.

2.4. SWiM-IRMS and dual-inlet IRMS

Values of $\delta^{13}C_{GDGT}$ are measured by Spooling Wire Microcombustion-IRMS (SWiM-IRMS; Sessions et al., 2005). Briefly, 1 μl of analyte is deposited on a pre-oxidized Ni wire which moves horizontally into a combustion furnace where it is combusted to CO_2, separated from H_2O in a Nafion drying tube, and enters the IRMS *via* an open split. Our system operates similarly to that of Sessions et al. (2005), with the following modifications for GDGTs: cleaning furnace, 950 °C; combustion furnace, 900 °C; and a ceramic combustion reactor with modified gas flow (Mohr et al., 2014). Each sample is analyzed in quintuplicate, at 30-s intervals.

High-precision $\delta^{13}C$ values for GDGT standards (C_{46} GTGT and crenarchaeol) were measured on large aliquots

of CO_2 prepared by closed-tube combustion (850 °C quartz tube, CuO 100 mg, 5 h), using dual-inlet VG Prism IRMS.

2.5. Ether cleavage and GC-IRMS

C_{40} biphytanes are cleaved from GDGTs using standard methods to form iodides in 55% HI, followed by reduction by $LiAlH_4$ in 1,4-dioxane (Hoefs et al., 1997; Pearson et al., 2001). Reaction times of 1 h, 2 h, and 3 h for both the lysis and reduction steps were tested; the best yield is obtained at 2 h, but there are no measurable isotopic differences between any of the times. Biphytane values of $\delta^{13}C$ ($\delta^{13}C_{biphy}$) are measured on a Thermo Delta V Advantage connected to a Trace GC Ultra *via* a GC Isolink interface operated at 990 °C (30 m × 0.25 mm, HP-5MS column); internal isotope standards are *n*-C_{38} and *n*-C_{41} alkanes.

2.6. Principal component analysis

Data for SBB were removed, due to a compromised result for the GDGT-[2/3] ratio caused by GDGT-3 signal near detection limits. All other samples were analyzed with respect to: individual compound $\delta^{13}C_{GDGT}$, latitude, longitude, water depth, $\delta^{13}C_{DIC}$ at 100 m, $\delta^{13}C_{DIC}$ at 500 m, $\delta^{13}C_{TOC}$, %TOC, C/N, GDGT-[2/3], TEX_{86}^{H}, TEX_{86}^{L}, SST, minimum [O_2] in the water column, depth of [O_2]min, and depth of maximum nitrate gradient (d[NO_3^-]/dz). PCA and cluster analysis were performed in Matlab R2015b with standardized data.

3. RESULTS

3.1. Precision and accuracy of $\delta^{13}C_{GDGT}$ measurements by SWiM-IRMS

The application of $\delta^{13}C_{GDGT}$ data to practical problems in (paleo)oceanography requires that the GDGT samples are sufficiently purified from background contamination, and that the isotope measurements are precise, accurate, and reproducible. We evaluated all of these factors systematically to develop quality control criteria.

3.1.1. GDGT Purification

Material that may not be compositionally related to GDGTs is present in minor amounts in the F1 fraction of the RP-HPLC purification (Fig. 1B; black trace). We minimize the presence of this exogenous material by limiting the total amount of starting extract to be no more than is needed for successful IRMS analysis. This reduces the risk of peak broadening and carryover of F1 material into F2. Post-purification GDGTs from F2 have no contamination detectable in their chromatograms, as seen in a co-injection of purified GDGT-0 and crenarchaeol (Fig. 1B; grey trace).

The resulting total CO_2 combustion yields from IRMS (peak area, *m*/*z* 44) (Fig. 2) always show a general pattern of F2 > F1, consistent with the APCI-MS detection of significantly more GDGT (F2) than the leading material (F1). The agreement between CO_2 combustion yield and APCI-MS total ion chromatograms (TIC) is linear (Fig. S1A),

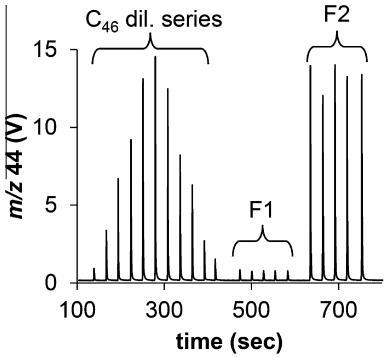

Fig. 2. Example SWiM-IRMS quantification of total CO_2 generated from a C_{46} GTGT standard dilution series and the F1 and F2 fractions of RP-HPLC-purified GDGTs. Peaks are spaced by 30 s, *i.e.*, quintuplicate $\delta^{13}C$ measurement of F2 in *ca.* 3 min.

and the scatter in these data is consistent with expectations that not all compounds have equal APCI-MS ionization potential, while combustion is quantitative. Thus the most accurate assessment of the relative carbon content of F1 and F2 is the combustion yield. In each sample, the F2:F1 ratio is always smaller for the minor GDGTs, relative to crenarchaeol and GDGT-0 (Fig. S1B). This reflects the lower concentrations of GDGTs-1, -2, and -3, relative to what are relatively constant F1 peaks in all GDGT fractions of a given sediment horizon. Carryover of background material into F2 is therefore of greater concern for the minor GDGTs.

We also evaluate the purity of each final F2 fraction by APCI-MS analysis. Using an empirical formula to convert between molecular ion abundance [M^+] and total ion abundance, we determine the fraction of TIC signal that can be assigned to the GDGT. This "purity" metric is high when F2:F1 is high (Fig. S1B). Based on broad evaluation of the total data set, and specifically on replicate analyses of our large-batch Carolina sample, we set stringency criteria for acceptable samples for SWiM-IRMS: an F2:F1 ratio ⩾ 5 and "purity" ⩾ 80% (Fig. S1B, area 1). Most of the cases of lower purity actually reflect co-elution and inclusion of other GDGTs (*e.g.*, GDGT-2 in the GDGT-1 fraction). The background of non-GDGT-related material is <5% in all final data.

3.1.2. SWiM-IRMS precision and accuracy

To ensure accuracy of $\delta^{13}C_{GDGT}$ data, we analyze a dilution series of the C_{46}-GTGT standard with every IRMS run (Fig. 2). Dilution series data are used to evaluate the combustion linearity (conversion to CO_2; $R^2 > 0.99$; Fig. S2A), to monitor the daily and long-term precision of $\delta^{13}C$ measurements (±0.25‰; Fig. S2B), and to apply absolute offset (accuracy) and blank corrections to the raw data to ensure that values from every run are standardized to the same reference frame.

To evaluate this approach, we purified two dilution series of crenarchaeol from the Carolina sediment. The results were compared to data from a large batch of a crenarchaeol standard previously prepared from this sediment and

double-purified (twice through the HPLC protocol) before analysis in triplicate by closed-tube combustion and dual-inlet IRMS (-18.51 ± 0.06‰). SWiM-IRMS data from the crenarchaeol dilution series (Fig. 3; June, July) and subsequent individual trials (Fig. 3; August, October) were analyzed using run-specific corrections derived from C_{46}-GTGT. The resulting SWiM-IRMS data converge on a mean value of −18.75‰, indicating a systematic offset of −0.25‰ between the continuous-flow and dual-inlet instruments. These constitute authentic, experimental replicates of all steps except for the initial solvent extraction. The SWiM-IRMS measurements for these replicates do not vary as a function of date or sample size, with the exception of one high-concentration sample that may have overloaded the combustion reactor, resulting in preferential combustion of ^{12}C (August sample).

Precision of the $\delta^{13}C_{GDGT}$ data is dependent on size, with samples containing <2 μgC in general having measurement precision *ca.* 0.4‰, while samples >2 μgC have measurement precision *ca.* 0.1–0.2‰; long-term precision of the C_{46}-GTGT standard is 0.25‰ (Fig. S2B). Precise analysis of samples by SWiM-IRMS is therefore limited by size considerations. We suggest a practical lower limit for $\delta^{13}C_{GDGT}$ analysis of 1 μg GDGT in the original sample.

3.1.3. Storage time series for Carolina large-batch GDGTs

Initially we explored whether purification and long-term storage of large batches of dissolved Carolina crenarchaeol and Carolina GDGT-0 would serve as suitable isotope standards. Such standards would need to remain soluble and free from contamination. Time-series trials of four aliquots of each standard – one each in 1:3 ethyl acetate/acetonitrile, 3:97 isopropanol/hexane, 100% CH_2Cl_2, and 100% ethyl acetate – were dissolved and their concentrations and $\delta^{13}C_{GDGT}$ values were measured for 45 days (Fig. S3). While the concentrations remained relatively stable, both compounds experienced a decrease in $\delta^{13}C_{GDGT}$ values of *ca.* 1‰ over the experiment, likely due to gradual contamination by volatiles or components of the vial caps (F-217/PTFE-lined Thermoset plastic; Qorpak). Based on these results, we conclude that large samples of GDGT and/or synthetic C_{46}-GTGT must be stored dry or in very concentrated stocks and only diluted to working concentration for APCI-MS and SWiM-IRMS within a few days of analysis.

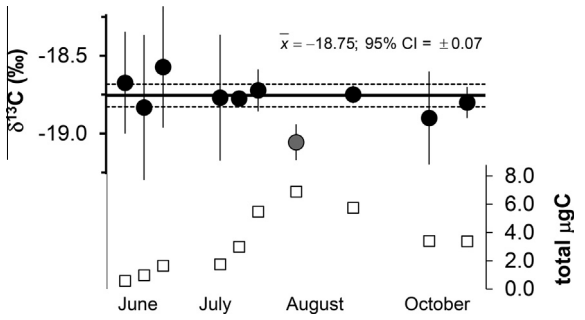

Fig. 3. Sequential record of the $\delta^{13}C$ measurements of Carolina crenarchaeol, monitored as a function of sample size and date analyzed. The average measurement precision is ±0.25‰.

3.2. Atlantic Ocean samples

The five samples from the western Atlantic have typical patterns of core GDGT distributions (Table 1), with warmer waters showing a decrease in GDGT-0 relative to crenarchaeol ([0/(0+Cr)]) and an increase in the ring index (RI) (Schouten et al., 2002) (Fig. 4A and B). As expected, the GDGT-2/3 ratio ([2/3]) is smallest at the shallowest Atlantic station (Carolina, 650 m) (Fig. 4C). The [2/3] ratios are higher at the deeper N. Atl. stations, yet are not highest at Cariaco, the deepest Atlantic site. When available, values of the BIT index of terrestrial input (Hopmans et al., 2004) are typical of sediments of primarily marine origin, although BIT values in some cases may underrepresent terrestrial carbon inputs (Walsh et al., 2008).

Temperatures calculated using the TEX_{86}^{H} index (Kim et al., 2010) for the southern stations (N. Atl. 18, Carolina, Cariaco) are within ±2.5 °C of annual mean SST (Fig. 4D). These values are within the expected error envelope for TEX_{86} regardless of calibration approach (Liu et al., 2009; Kim et al., 2010; Tierney and Tingley, 2014). When TEX_{86}^{H} is applied to the northern stations (N. Atl. 4, N. Atl. 11) it overestimates SSTs by up to 7.3 °C, outside the range of acceptable error. Temperatures calculated using TEX_{86}^{L} agree better for these stations, still overestimating local SSTs by 2.6–4.4 °C, but consistent with the idea that TEX_{86}^{L} is preferable at sites <15 °C.

The $\delta^{13}C_{GDGT}$ values for crenarchaeol from the N. Atl. 11, N. Atl. 18, and Cariaco samples all are statistically the same as the multiple trials of Carolina crenarchaeol (Fig. 3; Fig. 5; Table 1). The only Atlantic crenarchaeol sample that deviates is N. Atl. 4 (−19.6‰), the northernmost site. It is unknown whether this value indicates an undetected analytical artifact, or if it reflects a source of exogenous GDGTs specific to the location of Station 4 near the outlet of the Gulf of St. Lawrence, Canada. The value is inconsistent with the overall pattern of ^{13}C-enrichment in crenarchaeol relative to GDGT-0 for the Atlantic samples. The $\delta^{13}C_{GDGT}$ values measured for GDGT-0 from these five stations average -19.4 ± 0.2‰, with no GDGT-0 values significantly outside this range. Overall, the average $\delta^{13}C_{GDGT}$ value for GDGT-0 is 0.6‰ depleted in ^{13}C relative to crenarchaeol (excluding N. Atl. 4 crenarchaeol).

Values of $\delta^{13}C_{GDGT}$ for the minor GDGTs are the most strongly depleted in ^{13}C (Fig. 5; Table 1). The values for GDGT-1 and GDGT-2 from Carolina are 1.5‰ to 1.8‰ more negative than $\delta^{13}C_{GDGT}$ values for crenarchaeol. At N. Atl. 4 and N. Atl. 11, the value for GDGT-2 is only 0.3 to 0.6‰ more negative than the corresponding crenarchaeol and is similar to GDGT-0.

3.3. Pacific Ocean samples

The six samples from the Pacific Ocean also have typical patterns of core GDGT distributions (Table 1). These waters span a smaller gradient in annual mean SST

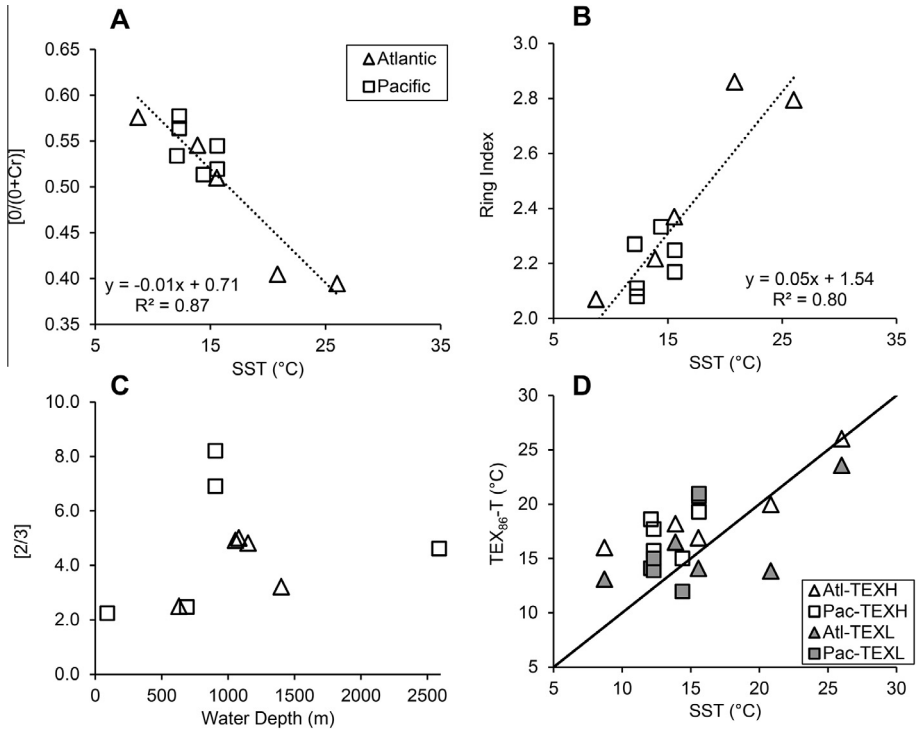

Fig. 4. GDGT indices for all samples. The relative abundances of GDGT-0 and crenarchaeol (A); the ring index (B); the GDGT-[2/3] ratio (C), and the TEX_{86}^{H} and TEX_{86}^{L}-calculated SSTs (Kim et al., 2010) (D).

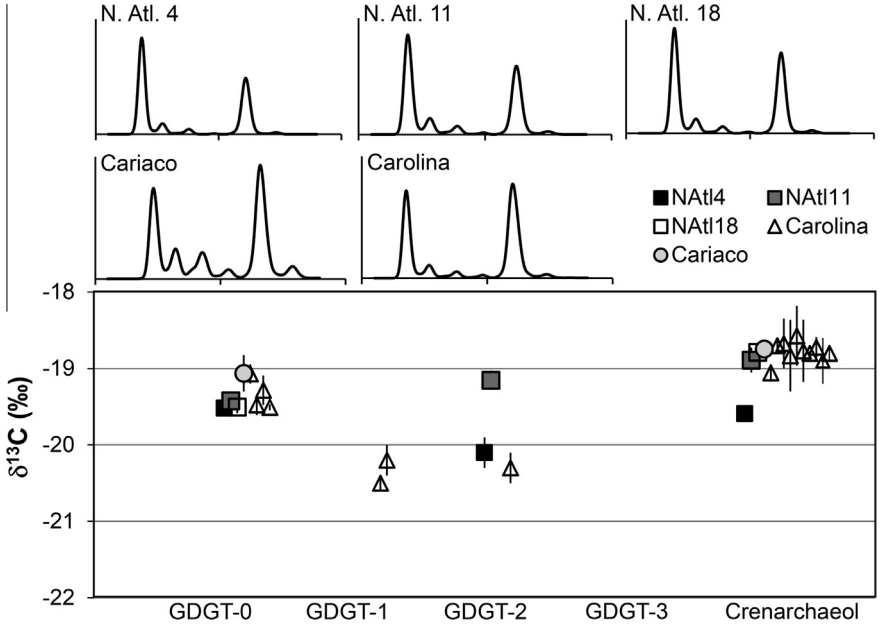

Fig. 5. Chromatograms and $\delta^{13}C_{GDGT}$ values for sediments from Atlantic Ocean locations.

(12 °C–16 °C), but the [0/(0+Cr)] ratios and values of the RI agree with the trends observed for the Atlantic stations (Fig. 4A,B). Values of [2/3] increase with depth only for the WA samples (Fig. 4C). The very high [2/3] value from SBB (off-scale, not shown in Fig. 4C) is an analytical artifact caused by the low abundance of GDGT-3 near detection limits. It could not be re-analyzed due to insufficient material. In contrast, the high [2/3] values of 7–8 for the two SMB samples are not affected by analytical issues and reflect a genuinely different [2/3] character of these sediments. Values of the BIT index are low for all samples in this set.

Temperatures calculated using TEX_{86}^{H} are higher than annual mean SST, although only WA-3 and WA-4 are >4 °C offset (Fig. 4D). Re-calculating the apparent temperatures using TEX_{86}^{L} brings all WA and SBB samples within 3 °C of annual mean SST. In contrast, using TEX_{86}^{L} to calculate temperatures for SMB results in poorer agreement, due to the strong dependence of TEX_{86}^{L} on the relative abundance of GDGT-2, which is disproportionally high in these samples.

In contrast to the Atlantic data, the Pacific data show patterns of $\delta^{13}C_{GDGT}$ values that are specific to each sample and are distinct between basin and open margin environments (Fig. 6; Table 1). The highest $\delta^{13}C_{GDGT}$ values are observed for the SMB 8-cm sample (average −18.5 ± 0.1‰), while the SMB 2-cm samples are more negative (average −19.0 ± 0.2‰), despite originating from the same core. These are bigger differences than can be explained by day-to-day variations in accuracy of SWiM-IRMS analyses and were repeatable (GDGT-2 replicate for SMB 8; Table 1). Values of $\delta^{13}C_{GDGT}$ for SBB averaged −19.1 ± 0.2‰. These numbers represent two adjacent core slices (5.5–6.0 cm and 6.0–6.5 cm), each processed independently from extraction through final SWiM-IRMS analyses, but yielding final $\delta^{13}C_{GDGT}$ values that agree within ±0.1‰ again demonstrating repeatability.

The WA samples are markedly different from the California Basin samples in both $\delta^{13}C_{GDGT}$ absolute values and patterns. GDGTs from the deepest, off-shore WA-7 location average −19.5 ± 0.2‰, with little variability between compounds. In contrast, the shallower margin locations, WA-3 and WA-4, are characterized by differences between individual GDGTs. As was seen in the Atlantic, crenarchaeol yields the most positive value (−20.5‰), relative to other GDGTs in each horizon. This pattern – especially for WA-4 (690 m water depth) – is similar to the offsets observed between individual GDGTs from the Atlantic Carolina sample (650 m water depth): GDGT-0 is 0.5‰ depleted and minor GDGTs are 2‰ depleted in ^{13}C relative to crenarchaeol. Yet despite the similarity in these relative patterns, the absolute values of $\delta^{13}C_{GDGT}$ for all of the WA samples are more negative than the Atlantic samples.

4. DISCUSSION

4.1. Influence of autotrophy vs. mixotrophy on marine archaeal lipids

Planktonic Archaea, specifically the Group I.1a Thaumarchaeota (Delong, 1992; Fuhrman et al., 1992; Spang et al., 2010), account for most of the ocean's ammonia oxidation (Francis et al., 2005; Könneke et al., 2005; Wuchter et al., 2006). To date, all pure and enrichment cultures of Thaumarchaeota (including the soil and hot springs Group I.1b (Pester et al., 2011), as well as marine taxa) are obligate carbon fixers, *i.e.*, they oxidize ammonia for energy and they fix inorganic carbon (Könneke et al., 2005; de la Torre et al., 2008; Hatzenpichler et al., 2008; Martens-Habbena et al., 2009; Santoro and Casciotti, 2011; Tourna et al., 2011; Qin et al., 2014). Widespread autotrophy among environmental Thaumarchaeota first was suggested based on the relatively ^{13}C-enriched C_{40} isoprenoid sidechains of GDGTs (Kohnen et al., 1992; Hoefs et al., 1997) and is supported by natural and label-enriched carbon isotope studies that indicate DIC is the primary carbon source (Pearson et al., 2001; Wuchter et al., 2003; Pitcher et al., 2011). For synthesis of archaeal lipids from dissolved inorganic carbon, the isotopic relationship between DIC and GDGTs is

$$\frac{\delta_{DIC}+1000}{\delta_{GDGT\_auto}+1000}=\alpha_{DIC/GDGT}=\frac{\varepsilon_{DIC/GDGT}}{1000}+1 \quad (1)$$

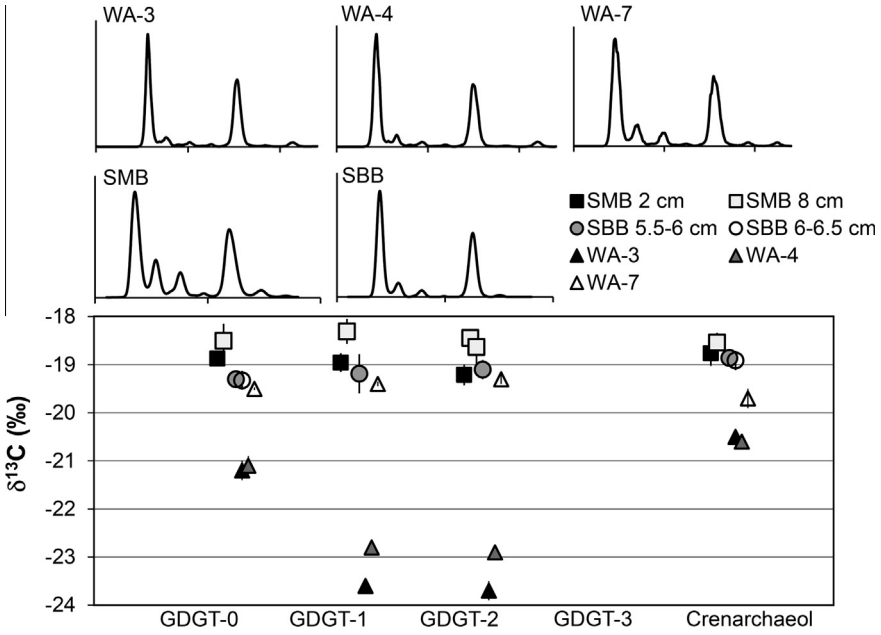

Fig. 6. Chromatograms and $\delta^{13}C_{GDGT}$ values for sediments from Pacific Ocean locations.

and between DIC and biphytanes is

$$\frac{\delta_{DIC}+1000}{\delta_{biphy\_auto}+1000}=\alpha_{DIC/biphy}=\frac{\varepsilon_{DIC/biphy}}{1000}+1. \quad (2)$$

The difference between $\varepsilon_{DIC/GDGT}$ and $\varepsilon_{DIC/biphy}$ is the presence/absence of glycerol moieties.

To date, evidence suggests that $\varepsilon_{DIC/GDGT}$ and $\varepsilon_{DIC/biphy}$ are likely to be relatively invariable. Thaumarchaeota fix carbon from HCO_3^-, the quantitatively dominant fraction of DIC, and should not be subject to the [$CO_2(aq)$]-dependent isotope fractionations experienced by phytoplankton (*e.g.*, Laws et al., 1995). Consistent with the idea that changes in inorganic carbon availability do not affect fractionation, values of ε for *N. maritimus* do not vary as a function of HCO_3^- concentration ($\varepsilon_{DIC/biphy}=19.7\pm0.2‰$; $\varepsilon_{DIC/biomass}=19.85\pm0.06‰$; Könneke et al., 2012). In the archaeal 3-hydroxypropionate/4-hydroxybutyrate (3HP/4HB) pathway (Berg et al., 2007; Walker et al., 2010; Könneke et al., 2014), one molecule of acetyl-CoA is fixed from 2 molecules of HCO_3^-. Acetyl-CoA, the direct precursor of isoprene in these organisms, is formed as the primary metabolite, which also explains why $\delta^{13}C_{biphy\_auto}$ values are nearly identical to the total cell biomass (Könneke et al., 2012). If the dominant source of GDGTs to marine sediments is export of *autotrophic* biomass from the overlying water column, values of $\delta^{13}C_{GDGT}$ should be robust tracers for $\delta^{13}C_{DIC}$, offset by a constant biosynthetic factor $\varepsilon_{DIC/GDGT}$.

However, in addition to autotrophic metabolism, some cultured strains (*e.g.*, Qin et al., 2014; Stieglmeier et al., 2014) and natural communities (Ouverney and Fuhrman, 2000; Herndl et al., 2005; Ingalls et al., 2006) incorporate organic carbon substrates: they are obligate or facultative mixotrophs. Other strains cannot be grown without obligate bacterial partners, again suggesting dependence on unidentified metabolites (Santoro and Casciotti, 2011). Additionally it has been suggested that heterotrophic Euryarchaeota may also contribute to the water-column GDGT flux (Lincoln et al., 2014). This implies that some fraction of the carbon contained in GDGTs and biphytanes will derive from assimilated organic matter rather than DIC. This material will alter the observed values of $\delta^{13}C_{GDGT}$ and $\delta^{13}C_{biphy}$ relative to the expected autotrophic values. For now we assume the assimilated organic substrate(s) derive from material having average $\delta^{13}C$ composition equal to bulk water-column SPM, and define f_{mixo} as the fraction of carbon incorporated from this generic source:

$$\delta_{GDGT}=(1-f_{mixo})\left(\frac{\delta_{DIC}+1000}{\frac{\varepsilon_{DIC/GDGT}}{1000}+1}-1000\right)+f_{mixo}\delta_{SPM} \quad (3)$$

$$\delta_{biphy}=(1-f_{mixo})\left(\frac{\delta_{DIC}+1000}{\frac{\varepsilon_{DIC/biphy}}{1000}+1}-1000\right)+f_{mixo}\delta_{SPM}. \quad (4)$$

The *net environmental* values of $\delta^{13}C_{GDGT}$ and $\delta^{13}C_{biphy}$ therefore include the mixotrophic component and reflect the net fractionations ($\varepsilon_{net/GDGT}$ and $\varepsilon_{net/biphy}$):

$$\frac{\delta_{DIC}+1000}{\delta_{GDGT}+1000}=\frac{\varepsilon_{net/GDGT}}{1000}+1 \quad (5)$$

$$\frac{\delta_{DIC}+1000}{\delta_{biphy}+1000}=\frac{\varepsilon_{net/biphy}}{1000}+1. \quad (6)$$

The distinction between autotrophic and net values of ε is critical, because the following analysis shows that environmental values of $\delta^{13}C_{GDGT}$ and $\delta^{13}C_{biphy}$ are not consistent with exclusively autotrophic growth of the archaeal community, *i.e.*, the data confirm the importance of mixotrophy.

We begin by assuming that crenarchaeol is the compound least affected by exogenous sources, including *in-situ* sedimentary production and euryarchaeal inputs. Our large-batch sample of Carolina crenarchaeol has values of $\delta^{13}C_{GDGT}=-18.5‰$ and $\delta^{13}C_{biphy}=-19.5‰$ ($\pm0.2‰$; $n=6$ for $C_{40:3}$). The local value of $\delta^{13}C_{DIC}$, based on the average of 100–1000 m water from the four nearest stations (Schmittner et al., 2013), is 0.9‰ (Fig. S4). This estimate for DIC does not change significantly if the depth integration is modified to 100–500 m (0.9‰) or 100–300 m (1.0‰). The resulting environmental values are $\varepsilon_{net/GDGT}=19.8\pm0.3‰$ and $\varepsilon_{net/biphy}=20.8\pm0.2‰$ (Eqs. (5) and (6); Table 2). However, the isotopic values for the other GDGTs from Carolina are not constant, suggesting there could be some source mixing, and this source mixing may also affect the crenarchaeol to an unknown extent. Thus we also performed the same calculation using sample WA-7, the deepest sediment horizon (2589 m) and a sample for which all $\delta^{13}C_{GDGT}$ values are uniform (Table 1). The Pacific Ocean value of $\delta^{13}C_{DIC}$, based on the average of 100–1000 m water (Schmittner et al., 2013), is −0.3‰. Due to the steeper gradients in the Pacific, this estimate becomes systematically more positive if the depth integration is modified to 100–500 m (−0.1‰) or 100–300 m (0.0‰), so to be conservative we used $0.0\pm0.4‰$ for the calculations. The result for WA-7 is $\varepsilon_{net/GDGT}=19.9\pm0.4‰$. This value agrees with the Carolina calculation and suggests that neither of these samples is significantly compromised by material of non-planktonic origin (Table 2). We therefore suggest that $\varepsilon_{net/GDGT}=19.8‰$ is a good estimate for the total marine planktonic community.

These results for net environmental fractionation are not the same as found for a pure culture growing strictly autotrophically. Multiple replicates of *N. maritimus* yielded $\varepsilon_{DIC/biphy}=19.7\pm0.2‰$ (Könneke et al., 2012), significantly less fractionated than our environmental result of $\varepsilon_{net/biphy}=20.8\pm0.2‰$ (Table 2). Könneke et al. (2012) do not report a value for $\varepsilon_{DIC/GDGT}$, but because biphytanes are ^{13}C-depleted relative to GDGTs, glycerol moieties must be ^{13}C-enriched. By isotope mass balance, the glycerol units of crenarchaeol from the Carolina sample have $\delta^{13}C_{gly}=-4.8‰$, equivalent to $\varepsilon_{gly}=5.7\pm0.4‰$ (Table 2). This is similar to the value of $\varepsilon_{mannose}$ of 6.1‰ reported for *N. maritimus* (Könneke et al., 2012), suggesting that the glycerol component of GDGTs is isotopically similar to cell sugars. Applying our ε_{gly} result to the Könneke et al. (2012) data results in $\varepsilon_{DIC/GDGT}=18.7\pm0.4‰$ (Table 2). Alternatively, averaging our mass balance value for ε_{gly} with a measured value for glycerol from Peru Margin sedimentary

Table 2
Carbon isotope fractionation observed in autotrophic *N. maritimus* SCM1 compared to net total fractionation observed in crenarchaeol from core-top sediments.

	$\varepsilon_{DIC/biphy}$	$\varepsilon_{DIC/GDGT}$	ε_{gly}
Culture data (*N. maritimus*)	19.7 ± 0.2[a]	18.7 ± 0.4[c] 19.0 ± 3.6[b]	10.0 ± 3.5[b]
Sediment data	$\varepsilon_{net/biphy}$	$\varepsilon_{net/GDGT}$	ε_{gly}
Atlantic	20.8 ± 0.2	19.8 ± 0.3	5.7 ± 0.4
Pacific	*n/a*	19.9 ± 0.4	*n/a*
100% Autotrophic	$\delta^{13}C_{biphy\_auto}$	$\delta^{13}C_{GDGT\_auto}$	
Atlantic	-18.4 ± 0.3	-17.5 ± 0.4[c]	
Pacific	-19.3 ± 0.4	-18.4 ± 0.5[c]	
Net planktonic community[d]	$\delta^{13}C_{biphy}$	$\delta^{13}C_{GDGT}$	
Atlantic	-19.5 ± 0.2	-18.5 ± 0.2	
Pacific	-20.4 ± 0.4	-19.4 ± 0.2	

[a] Könneke et al. (2012) data.
[b] Calculated assuming glycerol represents the average of Könneke et al. (2012) sugar data, Lin et al. (2013) glycerol measurement, and glycerol from Carolina Margin crenarchaeol.
[c] Value calculated using only the glycerol value from Carolina Margin crenarchaeol.
[d] Net community predictions calculated assuming constant $\varepsilon_{net/biphy} = 20.8‰$ and $\varepsilon_{net/GDGT} = 19.8‰$.

GDGTs (Lin et al., 2013) and the average of all sugars from Könneke et al. (2012) would yield $\varepsilon_{DIC/GDGT} = 19.0 \pm 3.6‰$, *i.e.*, an expanded uncertainty, but equal value. We therefore take $\varepsilon_{DIC/GDGT}$ to be 18.7‰. These values of $\varepsilon_{DIC/GDGT}$ and $\varepsilon_{DIC/biphy}$ predict that strictly autotrophic GDGTs from the Atlantic would have $\delta^{13}C_{GDGT} = -17.5 \pm 0.4‰$ and $\delta^{13}C_{biphy} = -18.4 \pm 0.3‰$; while strictly autotrophic GDGTs from the Pacific would have $\delta^{13}C_{GDGT} = -18.4 \pm 0.5‰$ and $\delta^{13}C_{biphy} = -19.3 \pm 0.4‰$. These estimates are on average $\geqslant 1‰$ more ^{13}C-enriched than our observations.

If the autotrophic fractionation exhibited by *N. maritimus* is representative of the autotrophic component of carbon fixation in all Thaumarchaeota (an assumption that must be tested by future studies on other isolates), the results imply that the total environmental community does not grow by strict autotrophy. Crenarchaeol, and by extension all other GDGTs derived from the planktonic archaeal community, must contain a fraction of non-DIC-derived carbon. This is consistent with activity-based evidence that mixotrophy and/or heterotrophy contributes significantly to the metabolism of Archaea in the ocean (*e.g.*, Ouverney and Fuhrman, 2000; Herndl et al., 2005). Using Eq. (3), we can evaluate the relative fraction of net organic carbon assimilation (f_{mixo}) for Carolina crenarchaeol and the WA-7 GDGTs, the remainder being autotrophic. For SPM endmembers of −21 to −23‰ (Druffel et al., 1998; Hwang et al., 2009), the observed $\delta^{13}C_{GDGT}$ values require of f_{mixo} of 12–35% (Atlantic) or 17–48% (Pacific). Because these estimates are heavily dependent on the choice of $\delta^{13}C$ value for SPM, we suggest that 25% be used as a best estimate for f_{mixo} until more results are available from both laboratory and field studies. This choice is slightly higher than an independent estimate of *ca.* 20% mixotrophy calculated for a planktonic sample from near Hawaii (Ingalls et al., 2006). Future work should examine different taxa of Thaumarchaeota, as well as total mixed planktonic communities (including marine Euryarchaeota), to determine phylogenetic, spatial, temporal, or other environmental controls on the net value of f_{mixo}, as well as its variability.

4.2. Isotopic records of archaeal biphytanes

The experimental value of strictly autotrophic $\varepsilon_{DIC/biphy}$ (Könneke et al., 2012) and the range of contemporary marine $\delta^{13}C_{DIC}$ values (−1 to 2‰; Schmittner et al., 2013) would yield values of $\delta^{13}C_{biphy}$ in the range of −20 to –17‰, with a predicted average *ca.* −19‰. However, a review of existing literature indicates that even in the most confidently planktonic-influenced surface sediments, $\delta^{13}C_{biphy}$ values are consistently below this range. There are very few reported values $\geqslant -19‰$ (*c.f.*, Schouten et al., 2013). Instead, $\delta^{13}C$ values for biphytanes of Neogene and younger marine sediments are $-21.2 \pm 0.9‰$ for $C_{40:0}$ and $C_{40:1}$ and $-20.4 \pm 0.6‰$ for $C_{40:2}$ and $C_{40:3}$ (after curation to remove sediment horizons thought to be affected by methane cycling). These systematic 1–2‰ offsets from the autotrophic prediction confirm that our estimates for f_{mixo} and $\varepsilon_{net/biphy}$ are universally applicable in direction and approximately constant in magnitude, at least for analysis of archaeal lipids from recent marine sediments. In other locations, biphytanes are even more strongly ^{13}C-depleted and show large differences between $C_{40:3}$ (derived uniquely from crenarchaeol) and $C_{40:0}$, $C_{40:1}$, and $C_{40:2}$ biphytanes, especially in deposits affected by methane cycling (*e.g.*, Pancost et al., 2001; Wakeham et al., 2003; Hoffmann-Sell et al., 2011; Schubotz et al., 2011).

Some of the scatter in reported biphytane values may be due to analytical challenges. All of our biphytane values and the Könneke et al. (2012) samples were measured either on lipid extracts of cultured biomass or on purified, individual GDGTs, yielding GC chromatograms free from complications of co-eluting peaks. In comparison, chromatograms from sediment extracts may be quite complex, with possible

co-elution of non-related compounds (*e.g.*, Hoefs et al., 1997). In some cases this results in differences between $C_{40:2}$ and $C_{40:3}$ (dominantly sourced by the same parent compound, crenarchaeol) of $\geqslant 1‰$ (*e.g.*, Schouten et al., 1998, 2001; Stadnitskaia et al., 2008), although these cases are uncommon. It is also possible that there is a systematic isotope fractionation during ether cleavage, although our preliminary trials suggest an insignificant effect. Overall it seems likely that reported $\delta^{13}C_{biphy}$ values are relatively unbiased, although they do mix together the biphytanes from different parent GDGT structures that may originally have had different $\delta^{13}C$ values.

In sum, the available literature consistently shows that biphytanes are ^{13}C-poor relative to purely autotrophic biosynthesis, even if there remains some uncertainty and/or scatter in the absolute values. The data indicate that contributions from thaumarchaeal mixotrophy, euryarchaeal heterotrophy (*e.g.*, Iverson et al., 2012), or allochthonous sources are ubiquitous features of sedimentary records of archaeal lipids and must be considered for all interpretations of carbon isotope data. Here we confine the remainder of the discussion to GDGTs, rather than biphytanes, mindful that the discussion applies to both molecular classes.

4.3. Regional patterns of GDGT signals: testing the Atlantic vs. Pacific $\delta^{13}C_{DIC}$ proxy

Contributions from f_{mixo} can be accommodated within $\delta^{13}C_{DIC}$ proxy reconstructions. A constant $\varepsilon_{net/GDGT}$ (*i.e.*, relatively constant f_{mixo}) implies that values of $\delta^{13}C_{GDGT}$ should vary systematically with $\delta^{13}C_{DIC}$. To test this idea, we examined the SWiM-IRMS $\delta^{13}C_{GDGT}$ data for crenarchaeol from all locations (Table 1). Crenarchaeol is the compound most confidently sourced from Thaumarchaeota, while other GDGTs may have additional sources, including, but not necessarily limited to marine planktonic Euryarchaeota (Pearson and Ingalls, 2013; Schouten et al., 2013; Lincoln et al., 2014).

Our SWiM-IRMS value of $-18.75 \pm 0.25‰$ for Carolina crenarchaeol is near the lower bound of analytical uncertainty for the large-batch standard we prepared of this same material ($-18.51 \pm 0.06‰$; dual-inlet IRMS). We assume that the latter represents the more accurate value, indicating there may be a systematic negative bias in our SWiM-IRMS data of 0.2 to 0.3‰. Considering this bias, the crenarchaeol values from the Carolina, Cariaco, N. Atl. 18, and possibly the N. Atl. 11 sites (Fig. 5) all appear to agree with a $-18.5‰$ prediction for Atlantic margin GDGTs, based on $\varepsilon_{net/GDGT} = 19.8‰$ and $\delta^{13}C_{DIC} = 0.9‰$. Only the N. Atl. 4 site ($-19.6‰$) is significantly ^{13}C-depleted relative to expectations. This is a suspected analytical outlier, as the negative anomaly does not extend to other GDGTs measured from the same sediment. Overall, crenarchaeol across the wide latitudinal range of Atlantic margin sediments agrees with the idea of a constant f_{mixo}, with *ca.* 75% of the carbon fixed from DIC and the remainder from organic carbon assimilation from average SPM.

In contrast, crenarchaeol values from most of the Washington and California margin samples are not robust with respect to this model. Only WA-7, the deepest, farthest off-shore site (2589 m), reflects the estimated $\varepsilon_{net/GDGT} = 19.8‰$, above. This is the most strongly marine-dominated location of the Pacific samples, farthest from the influence of the nearby Columbia River watershed, and on the open margin rather than from within a suboxic basin. The other two WA samples are from shallower locations influenced by river-transported sediments. Terrigenous material contributes up to 60% of carbon in these sediments, as evidenced by low bulk $\delta^{13}C$ values (average $-24‰$), a high C/N ratio (average 14), and the presence of lignin phenols, although the BIT index is low (Prahl et al., 1994; Walsh et al., 2008). Crenarchaeol ($-20.5‰$, $-20.6‰$), as well as the other GDGTs from these samples (next section), is consistent with a partially terrigenous or riverine source.

The most inconsistent results are for the California basins, SMB and SBB. Their $\delta^{13}C$ values for crenarchaeol are more positive than expectations: as high as $-18.5‰$ in the case of the SMB 8-cm horizon, which is well above a predicted Pacific value of $-19.4‰$ (Table 2). To be explained by water-column export, either 100% of the crenarchaeol flux would have to come from the upper 50 m of the water column, where $\delta^{13}C_{DIC}$ is more positive, or the value of $\varepsilon_{net/GDGT}$ would have to be identical to $\varepsilon_{DIC/GDGT}$, *i.e.*, $f_{mixo} = 0$ among the local archaeal community. The first option is disallowed, given the negative ^{14}C signatures for biphytanes and GDGTs from these basins (Pearson et al., 2001; Shah et al., 2008), and the second option is biologically unlikely, as the original data suggesting archaeal mixotrophy were obtained from samples collected in California waters (Ouverney and Fuhrman, 2000) and other recent Pacific Ocean isolates demonstrate obligate mixotrophy (Qin et al., 2014). Similar to the near-shore WA samples, again the more likely cause of the isotopic discrepancies is an extra, exogenous source of GDGTs to these enclosed, near-shore basins.

Overall, our $\delta^{13}C_{GDGT}$ data for crenarchaeol are consistent with the idea that in young sediments dominated by marine influence, planktonically-derived GDGTs have a relatively constant biological fractionation ($\varepsilon_{GDGT\_net} = 19.8‰$) that reflects the balance of an isotope effect relative to DIC ($\varepsilon_{DIC/GDGT} = 18.7‰$), plus a quantitatively-significant input of organic carbon uptake (SPM from -21 to $-23‰$, *ca.* 25% of carbon). The challenges for further interpretation, however, are that not only does this result apply *only to open margin sites* away from river systems, it also applies *only to crenarchaeol* (Fig. 5, Fig. 6). Significantly different $\delta^{13}C_{GDGT}$ values within the same sediment sample effectively require that there be multiple sources for GDGTs. All samples of GDGT-0 from the Atlantic are ^{13}C-depleted relative to crenarchaeol, possibly reflecting a component of terrigenous or *in-situ* sedimentary influence, or contribution from planktonic, heterotrophic Euryarchaeota rich in GDGT-0 and assimilating fractionally more carbon from SPM rather than DIC. The values for GDGTs -1 and -2 are even more strongly ^{13}C-depleted in these samples, implying they are the most strongly affected by these alternate sources. Samples of GDGT-0 from the Pacific, in contrast, vary with respect

to the type of location. All GDGTs from the off-shore WA-7 sample are within error of the −19.4‰ prediction based on $\varepsilon_{net/GDGT}$. All GDGTs from the SMB 8-cm sample appear to be influenced by a ^{13}C-enriched source, as do the SMB 2-cm and SBB samples. Finally, the most extreme results come from the WA-3 and WA-4 shallow sites, where the GDGT-0, -1, and -2 values all are too ^{13}C-depleted to come exclusively from the water column. These GDGTs must have exogenous inputs, either allochthonous (*e.g.*, Smittenberg et al., 2005), *in-situ* heterotrophic (*e.g.*, Biddle et al., 2006), or autotrophic, incorporating ^{13}C-depleted DIC from pore waters or other ^{13}C-depleted waters (*e.g.*, Schubotz et al., 2011).

4.4. Evaluating exogenous contributions by isotope mass balance

To evaluate these patterns quantitatively, we examined the data for individual GDGTs using isotope mass balance. In all cases, each sample is assumed to be a 2-component mixture – marine GDGTs (defined as −18.5‰ Atlantic, −19.4‰ Pacific) plus an exogenous component:

$$\delta_{tot} = f_{mar}\delta_{mar} + f_{exo}\delta_{exo} \quad (7)$$

For the Atlantic samples, the exogenous input of GDGTs is assumed to be derived from a terrigenous (soil, lacustrine, or estuarine) endmember. The δ^{13}C value of this material is unknown, so we solved f_{exo} for values of δ_{exo} between −29‰ and −23‰. The lower boundary is set by a direct measurement of the δ^{13}C value of total Carolina TLE, while the upper boundary is taken from data for archaeal biphytanes from terrigenous sources (Pearson et al., 2004; Smittenberg et al., 2005; Sinninghe Damsté et al., 2009). In this scenario, the exogenous component accounts for 18–41% of Carolina GDGT-1 and -2, but only 2–6% of crenarchaeol (Table 3). The results for the other samples from the Atlantic are similar, suggesting the following approximation: crenarchaeol, GDGT-0, and the minor GDGTs are *ca.* 5%, 10%, and 25% exogenous, respectively. This calculation is not the same as the calculation of analytical purity (Section 3.1.1), which was aimed at detecting non-GDGT material in the samples (<5%). Here the estimates of f_{exo} indicate the fraction of the GDGT itself that derives from other sources. In agreement with this, f_{exo} and the "purity" score are not significantly correlated ($R^2 = 0.07$).

For isotope mass balance, we treat the WA samples similarly. The minimum value of the exogenous endmember ($\delta_{exo} = -29‰$) is defined as the average of regional higher plant *n*-alkane values (Prahl et al., 1992) and total organic matter (Prahl et al., 1994; Walsh et al., 2008). The maximum value of δ_{exo} cannot be the same as used above, because data from GDGT-1 and GDGT-2 from WA-3 are more negative than this value; instead we choose −24‰, consistent with fjord data from Smittenberg et al. (2005). We also note that preliminary measurements of branched bacterial GDGTs (brGDGTs; Weijers et al., 2006) from these samples yield δ^{13}C values of −26‰. Under these constraints, there is no significant fraction of exogenous GDGTs in WA-7. In the WA-3 and WA-4 samples, the fraction of exogenous material is very high, estimated to be 35–93% for the minor GDGTs (Table 3). This likely reflects the location of these sediments near the outlet of the Columbia River, consistent with the idea that isoprenoid GDGTs from terrestrial sources may be transported to marine systems (*e.g.*, Kim et al., 2006); yet here the BIT index is not a good indicator of the relative importance of this endmember, as has been shown previously (Walsh et al., 2008).

The most challenging samples to interpret are those from the California basins. In this region there are sediments of Plio/Pleistocene age, outcrops of the well-studied Miocene Monterey Shale (*e.g.*, Schouten, 1995; Schouten et al., 1998), and thick (>1000 m) sections of Cretaceous deposits with significant exposures in the Santa Monica mountains (Yerkes et al., 1965). The average δ^{13}C value of $C_{40:2}$ and $C_{40:3}$ biphytanes for the non-dolomitic (*i.e.*, not affected by methane cycling) strata of the Monterey Shale is −20.7‰, indistinguishable from contemporary or Plio/Pleistocene inputs (Hoefs et al., 1997; Schouten et al., 1998; Hoffmann-Sell et al., 2011). In contrast, weathering of the Cretaceous sections may yield ^{13}C-enriched biphytanes, similar to the −17.8‰ average of Kuypers et al. (2001), which would equate to *ca.* −17‰ for the weathering of corresponding GDGTs. We therefore calculated the potential effect on SMB/SBB sedimentary GDGTs

Table 3
The estimated fraction of non-planktonic GDGTs (exogenous; f_{exo}) present in each sediment sample.

	z (m)	f_{exo} (%)			δ_{exo} (‰)
		GDGT-0	GDGT-1&2	Cren	
Carolina	650	8–19%	18–41%	2–6%	−29 to −23
Cariaco	1400	6–13%	*n/a*	2–4%	−29 to −23
N. Atl.[a]	1055–1150	9–21%	11–26%	3–8%	−29 to −23
WA-7	2589	1–2%	0%	3–7%	−29 to −24
WA-4	690	18–37%	35–76%	13–26%	−29 to −24
WA-3	91	19–39%	44–93%	11–24%	−29 to −24
SBB/SMB 2	600–905	2–21%	4–17%	9–25%	−17
SMB 8	905	17–38%	17–46%	17–38%	−17

Results are constrained by a range of δ^{13}C values for the hypothetical endmember (δ_{exo}).
Generally, crenarchaeol is the compound least influenced by f_{exo}, while minor GDGTs and near-shore locations are more strongly influenced.
[a] All N. Atl. stations treated as one, with the −19.6‰ outlier for N. Atl. 4 excluded.

of an exogenous endmember having a Cretaceous $\delta^{13}C$ value. The resulting estimates are that 2–38% of GDGTs in the California system are exogenous. However, such an estimate ignores the potential inputs of GDGTs from more recent terrigenous sources such as soils, including those influenced by the presence of C_4 vegetation. Previous radiocarbon studies of biphytanes, GDGTs, *n*-alkanes, and total organic matter from these sediments show that the archaeal lipids are not more than 10–15% derived from fossil sources (Pearson et al., 2001; Shah et al., 2008) and that pre-aged detrital and plant-derived carbon sources also are significant inputs (Bauer et al., 1995; Pearson and Eglinton, 2000; Mollenhauer and Eglinton, 2007). Refining the ^{13}C mass balance using ^{14}C constraints suggests the GDGT sources may be approximately 80% planktonic, 10% fossil, and 10% pre-aged detrital of unknown source and endmember ^{13}C value. This would be consistent with results in Table 3, although not yet completely explained. Overall, however, it appears that the primary reason for anomalous $\delta^{13}C_{GDGT}$ values in SMB/SBB is the unusual nature of the exogenous source(s), rather than a high abundance of this material.

4.5. Implications for paleoceanography: TEX_{86} and carbon cycle reconstructions

Our $\delta^{13}C_{GDGT}$ results show that GDGTs in most shelf/slope sediments are influenced by exogenous sources, possibly introducing both temporal (*e.g.*, eroded sediments) and environmental (*e.g.*, terrigenous *vs.* marine) complications to the interpretation of paleorecords.

The influence of these effects on paleotemperature reconstructions is a function of the difference between the TEX_{86} value of the exogenous source and the TEX_{86} signal of the local water column. Considering that the non-local fraction of minor GDGTs may be several tens of percent (Table 3), we calculated the error in the resulting SST (ΔSST, calculated using TEX_{86}^{H}) as a function of f_{exo} from 0 to 80% and the difference in TEX_{86} ratio between local and exogenous inputs ($TEX_{86(local)} - TEX_{86(exo)}$). Results are shown for a hypothetical sediment having a local TEX_{86} ratio of 0.5 plus an exogenous input with a TEX_{86} ratio between 0.3 and 0.7 (Fig. 7). Inputs with TEX_{86} ratios of 0.3–0.7 would span most of the natural variability in TEX_{86} observations (Tierney and Tingley, 2015). The resulting errors in calculated SSTs (ΔSSTs) therefore span most of the expected outcomes and can be considered reasonable estimates of the maximum potential bias caused by non-local, non-planktonic sources of GDGTs. The error calculation is asymmetric, *e.g.*, at $f_{exo} = 75\%$, ΔSST is +7.8 °C and −10.6 °C, for TEX_{86} values for f_{exo} of 0.7 and 0.3, respectively. This is due to the logarithmic formulation of TEX_{86}^{H} (Kim et al., 2010). In general, however, the effect of f_{exo} on calculated values of TEX_{86}^{H} is surprisingly small. For sediments with f_{exo} <50% for the minor GDGTs (*e.g.*, all of the Atlantic samples; Table 3), errors in the resulting SSTs would be no more than +5.4 °C to −6.6 °C; while if f_{exo} is <30%, errors would be +3.4 °C to −3.8 °C. The latter is within the expected error of ±3–5 °C for the most recent TEX_{86} calibrations (Kim et al., 2010; Tierney and Tingley, 2014). Indeed, some of the scatter in these calibrations may be due to the variable input of non-local GDGTs. Since all of our samples other than WA-3, WA-4, and the SMB 8-cm sample meet the criterion of f_{exo} <30% for the minor GDGTs, it appears that open marine sediments generally contain insufficient exogenous material to cause bias in TEX_{86}-calculated paleorecords generated from such locations.

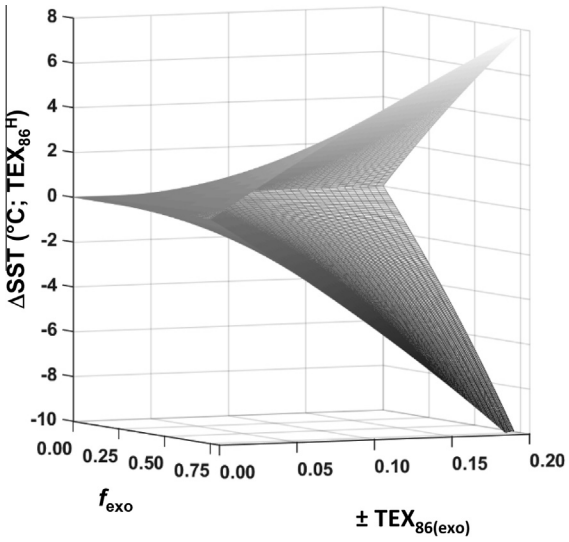

Fig. 7. Error in TEX_{86}^{H}-calculated SSTs caused by the presence of exogenous GDGTs. The potential error in reconstructed SST is shown for 0–75% exogenous overprinting of an original planktonic ("true") signal by an exogenous source that differs by up to ±0.2 in its TEX_{86} ratio.

The challenges for reconstructing $\delta^{13}C_{DIC}$ clearly are much larger. Site selection must be confined to locations dominated by marine planktonic inputs, ideally with f_{exo} <10%. Such sites potentially are limited to non-basinal deposits recovered from ⩾1000 m water depth (*e.g.*, the Atlantic margin sites and WA-7), although more study is needed to better determine if depth is the most appropriate metric for determining the cutoff. Analytically the most precise and accurate results are obtained by isolating pure crenarchaeol, followed by analysis by SWiM-IRMS. Since SWiM-IRMS is not currently available to most users, ether cleavage of pre-purified crenarchaeol followed by analysis by GC-IRMS is the recommended strategy. This will yield values of $\delta^{13}C_{biphy}$ that can then be converted to $\delta^{13}C_{DIC}$ values using $\varepsilon_{net/biphy}$. The quality of these interpretations depends most strongly on the variability of $\varepsilon_{net/biphy}$, which is a function of f_{mixo} and the $\delta^{13}C$ value of assimilated organic carbon (here assumed to be marine SPM, *i.e.*, bulk planktonic biomass). Also, our calculations assume that $\varepsilon_{DIC/biphy}$ is constant (to ±0.2‰), which to date has been tested only in one taxon (Könneke et al., 2012). This must be examined in more detail – for example, as a function of temperature, and in different strains of ammonia-oxidizing Thaumarchaeota. Future studies on a wider range of sediment core-tops will allow all of these variables to be studied in greater detail.

In addition to a lack of data on the metabolic (and therefore isotopic) diversity of natural communities of marine Archaea, there remain other significant uncertainties in our estimates of exogenous GDGT contributions to sediments. *N. maritimus* is a group I.1a Thaumarchaeon, yet exogenous GDGTs may be contributed by the group I.1b soil-dwelling group (*e.g.*, *N. viennensis*; Pester et al., 2011). Studies of carbon isotope fractionation should be expanded to this clade, as well as to samples of mixed natural communities taken directly from the marine water column. The precision and accuracy of our measurement method is sufficient to distinguish small changes in ^{13}C composition of endmember carbon sources, both for the exogenous material and the *in situ* GDGTs. The former may be affected by changes in erosional patterns, while the latter is potentially complicated by the *ca.* 1‰ decrease in surface ocean $\delta^{13}C_{DIC}$ in recent decades (the Suess effect; Swart et al., 2010), although this effect should bias all of our samples equally. Finally, the most difficult challenge for assessing uncertainties in the exogenous contribution is to distinguish sedimentary *in-situ* production from allochthonous material. When *in-situ* production is distinct in ^{13}C composition (*e.g.*, Schubotz et al., 2011), these sources are easily detected, but in the majority of cases the *in-situ* production may be indistinguishable from general heterotrophic biomass (*e.g.*, Biddle et al., 2006).

Overall, it remains possible that several complicated or multi-variable factors will be found to affect the overall patterns of $\delta^{13}C_{GDGT}$ values. To test for environmental patterns, we performed a PCA analysis on the $\delta^{13}C_{GDGT}$ data and other water-column and sediment data gathered from the literature for these locations. Five factors explained >90% of the variance (Fig. 8). Interestingly, the variance in $\delta^{13}C_{GDGT}$ values was not explained well by differences in $\delta^{13}C_{TOC}$, water column depth, sediment C/N ratio, or other likely sediment source indicators. These sediment source indicators all mapped to principal components PC2 and PC3 and covaried with each other. PC2 and PC3 also clustered with PC1, the component on which the temperature indicators were weighted most heavily (SST, TEX_{86}^H, TEX_{86}^L); interestingly, %TOC also clustered with temperature. Instead, $\delta^{13}C_{GDGT}$ values appear to covary most strongly with [2/3], suggesting that the best predictor for $\delta^{13}C_{GDGT}$ values is changes in relative abundances of the GDGTs themselves – *i.e.*, GDGT source mixing cannot be predicted from C/N or %TOC, but when [2/3] changes, values of $\delta^{13}C_{GDGT}$ also change (PC4). The environmental variable that most strongly co-varies with these GDGT source indicators is the water column nutrient gradient (PC5), here parameterized as the depth of the steepest gradient in nitrate regeneration ($d[NO_3^-]/dz$). This is consistent with hypotheses that depth-dependent physiological and/or population changes are important influences on the distribution of marine GDGTs (*e.g.*, Turich et al., 2007; Kim et al., 2016). Future work to measure values of δ^3C_{GDGT} directly from the water column will help determine whether different communities show different isotope effects, and if those values co-vary with changes in GDGT-[2/3], TEX_{86}, and other GDGT ratios.

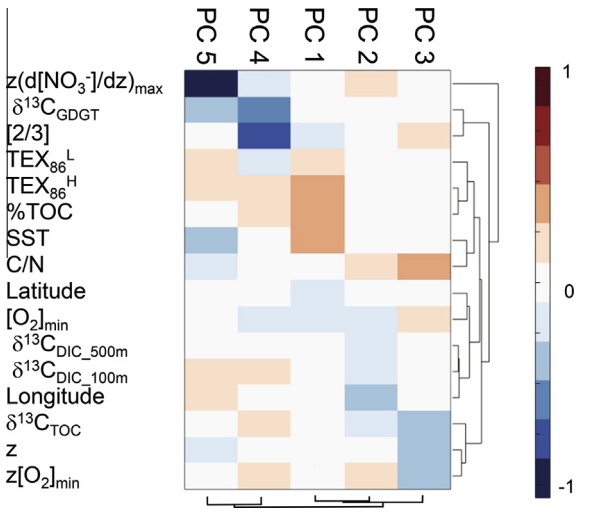

Fig. 8. Cluster diagram of the five principal components that explain >90% of the variance among $\delta^{13}C_{GDGT}$, latitude, longitude, z (m), SST (°C), TEX_{86}^H-SST, TEX_{86}^H -SST, %TOC, $\delta^{13}C_{TOC}$, C/N, GDGT-[2/3], depth of the O_2-minimum (m), $[O_2]_{min}$, depth of maximum nitrate regeneration ($d[NO_3^-]/dz$), $\delta^{13}C_{DIC}$ at 100 m, and $\delta^{13}C_{DIC}$ at 500 m. Environmental data were compiled from the literature (Tan and Strain, 1979, 1983; Walsh et al., 1985; Blair et al., 1994; Prahl et al., 1994; Pearson, 1999; Thomas et al., 2002; Mollenhauer and Eglinton, 2007; Drenzek, 2007) and from public databases (World Ocean Atlas, https://www.nodc.noaa.gov/OC5/woa13/; the CARIACO project, http://imars.usf.edu/cariaco; Calcofi Cruise 9610 Hydrographic Report, http://www.calcofi.org/data/data_reports/1990s/1996/9610_hyd.html).

5. CONCLUSIONS AND FUTURE WORK

Modern marine sediments have variable $\delta^{13}C$ values of GDGTs, both among individual GDGTs extracted from the same sediment, as well as among different locations on the same continental margin. The cause in both cases appears to be different fractional contributions from multiple sources, including – but not necessarily limited to – export of planktonic material from the water column and transport of weathered terrestrial sources (either soils or ancient sediments). The suite of samples studied here enables several preliminary conclusions, each of which will require additional examination:

(a) Mixotrophy and/or heterotrophy is a universal feature of the net archaeal community that contributes GDGTs to sediments. The $\delta^{13}C$ values observed for sedimentary GDGTs and biphytanes are too ^{13}C-depleted relative to DIC to be compatible with the measured isotope effect for obligate autotrophy (Könneke et al., 2012). Further surveys of $\delta^{13}C$ values for biphytanes and GDGTs will help define regional and/or depositional patterns.

(b) Accurate reconstruction of $\delta^{13}C_{DIC}$ values will require more study of environmental isolates or enrichments of both planktonic Thaumarchaeota and Euryarchaeota to refine the relationship between

the net carbon isotope fractionation ($\varepsilon_{net/GDGT}$) and the autotrophic fractionation ($\varepsilon_{DIC/GDGT}$), the difference being assimilation of organic carbon.

(c) Archaeal C_{40} biphytanes are ^{13}C-depleted relative to core GDGTs, indicating the glycerol moieties are ^{13}C enriched. This is consistent with a metabolic link between sugar metabolism and the glycerol-precursor metabolite, dihydroxyacetone phosphate (*c.f.*, Pearson, 2014), and is supported by small measured isotope effects for sugar head-groups and glycerol moieties of GDGTs (Könneke et al., 2012; Lin et al., 2013).

(d) Although exogenous GDGT sources to sediments are common, especially in shallow environments and/or in marginal basins, the effect of this material on TEX_{86}-reconstructed SSTs is within calibration uncertainty when it contributes <30% of the total GDGT accumulation. All of the open margin, non-river-affected samples in our present study meet this criterion.

(e) The presence of exogenous GDGTs has a variable and potentially large effect on the ability to reconstruct past values of $\delta^{13}C_{DIC}$. The use of biphytanes and/or GDGTs for understanding the marine carbon cycle will be limited to cores in which the organic matter flux is strongly marine, *i.e.*, either biogenic sediments or distant shelf/slope environments.

ACKNOWLEDGEMENTS

We thank Associate Editor Elizabeth Canuel and four anonymous reviewers for their valuable feedback. The following people provided access to samples and cruises: D. DeMaster (R/V Seward Johnson cruise, 1998; Carolina Margin sediment), K. Hughen and N. Drenzek (Cariaco; NSF OCE-0137005 and DEB-0447281), F. Prahl and S. Wakeham (Washington Margin sediments), Ellen Druffel (SMB/SBB sediments), and Tim Eglinton (N. Atlantic Line W cruise, 2010). Susan J. Carter provided laboratory assistance, and we benefitted from discussions with Jed Fuhrman, Sabine Lengger, Rich Pancost, Kate Freeman, and Ed DeLong. Funding was provided by the Gordon and Betty Moore Foundation and NSF (OCE-1129343 and EAR-1349126) (to A.P.), by the Deutsche Forschungsgemeinschaft (KU2842/1-1; to S.K.), and the Harvard University Center for the Environment (to Y.Z.).

APPENDIX A. SUPPLEMENTARY DATA

Supplementary data associated with this article can be found, in the online version, at http://dx.doi.org/10.1016/j.gca.2016.02.034.

REFERENCES

Basse A., Zhu C., Versteegh G. J. M., Fischer G., Hinrichs K. U. and Mollenhauer G. (2014) Distribution of intact and core tetraether lipids in water column profiles of suspended particulate matter off Cape Blanc, NW Africa. *Org. Geochem.* **72**, 1–13.

Bauer J. E., Reimers C. E., Druffel E. R. M. and Williams P. M. (1995) Isotopic constraints on carbon exchange between deep-ocean sediments and sea-water. *Nature* **373**, 686–689.

Berg I. A., Kockelkorn D., Buckel W. and Fuchs G. (2007) A 3-hydroxypropionate/4-hydroxybutyrate autotrophic carbon dioxide assimilation pathway in archaea. *Science* **318**, 1782–1786.

Biddle J. F., Lipp J. S., Lever M. A., Lloyd K. G., Sorensen K. B., Anderson R., Fredricks H. F., Elvert M., Kelly T. J., Schrag D. P., Sogin M. L., Brenchley J. E., Teske A., House C. H. and Hinrichs K. U. (2006) Heterotrophic Archaea dominate sedimentary subsurface ecosystems off Peru. *Proc. Natl. Acad. Sci. U.S.A.* **103**, 3846–3851.

Bijl P. K., Houben A. J. P., Schouten S., Bohaty S. M., Sluijs A., Reichart G. J., Sinninghe Damsté J. S. S. and Brinkhuis H. (2010) Transient middle Eocene atmospheric CO_2 and temperature variations. *Science* **330**, 819–821.

Blair N. E., Plaia G. R., Boehme S. E., Demaster D. J. and Levin L. A. (1994) The remineralization of organic carbon on the North Carolina continental slope. *Deep Sea Res. Part II* **41**, 755–766.

Church M. J., Wai B., Karl D. M. and DeLong E. F. (2010) Abundances of crenarchaeal *amoA* genes and transcripts in the Pacific Ocean. *Environ. Microbiol.* **12**, 679–688.

de la Torre J. R., Walker C. B., Ingalls A. E., Könneke M. and Stahl D. A. (2008) Cultivation of a thermophilic ammonia oxidizing archaeon synthesizing crenarchaeol. *Environ. Microbiol.* **10**, 810–818.

Delong E. F. (1992) Archaea in coastal marine environments. *Proc. Natl. Acad. Sci. U.S.A.* **89**, 5685–5689.

Drenzek N. J. (2007) *The Temporal Dynamics of Terrestrial Organic Matter Transfer to the Oceans: Initial Assessment and Application* Ph.D. Thesis. MIT/WHOI Joint Program, Woods Hole, MA.

Druffel E. R. M., Griffin S., Bauer J. E., Wolgast D. M. and Wang X. C. (1998) Distribution of particulate organic carbon and radiocarbon in the water column from the upper slope to the abyssal NE Pacific ocean. *Deep Sea Res. Part II* **45**, 667–687.

Elling F. J., Könneke M., Lipp J. S., Becker K. W., Gagen E. J. and Hinrichs K. U. (2014) Effects of growth phase on the membrane lipid composition of the thaumarchaeon *Nitrosopumilus maritimus* and their implications for archaeal lipid distributions in the marine environment. *Geochim. Cosmochim. Acta* **141**, 579–597.

Elling F. J., Könneke M., Greve A., Mußmann M. and Hinrichs K.-U. (2015) Influence of temperature, pH, and salinity on membrane lipid composition and TEX_{86} of marine planktonic thaumarchaeal isolates. *Geochim. Cosmochim. Acta* **171**, 238–255.

Francis C. A., Roberts K. J., Beman J. M., Santoro A. E. and Oakley B. B. (2005) Ubiquity and diversity of ammonia-oxidizing archaea in water columns and sediments of the ocean. *Proc. Natl. Acad. Sci. U.S.A.* **102**, 14683–14688.

Fuhrman J. A., McCallum K. and Davis A. A. (1992) Novel major archaebacterial group from marine plankton. *Nature* **356**, 148–149.

Hatzenpichler R., Lebedeva E. V., Spieck E., Stoecker K., Richter A., Daims H. and Wagner M. (2008) A moderately thermophilic ammonia-oxidizing crenarchaeote from a hot spring. *Proc. Natl. Acad. Sci. U.S.A.* **105**, 2134–2139.

Hernandez-Sanchez M. T., Woodward E. M. S., Taylor K. W. R., Henderson G. M. and Pancost R. D. (2014) Variations in GDGT distributions through the water column in the South East Atlantic Ocean. *Geochim. Cosmochim. Acta* **132**, 337–348.

Herndl G. J., Reinthaler T., Teira E., van Aken H. and Veth C., et al. (2005) Contribution of Archaea to total prokaryotic production in the deep Atlantic Ocean. *Appl. Environ. Microbiol.* **71**, 2303–2309.

Hoefs M. J. L., Schouten S., deLeeuw J. W., King L. L., Wakeham S. G. and Sinninghe Damsté J. S. S. (1997) Ether lipids of

planktonic archaea in the marine water column. *Appl. Environ. Microbiol.* **63**, 3090–3095.

Hoffmann-Sell L., Birgel D., Arning E. T., Follmi K. B. and Peckmann J. (2011) Archaeal lipids in Neogene dolomites (Monterey and Sisquoc Formations, California) – Planktic versus benthic archaeal sources. *Org. Geochem.* **42**, 593–604.

Hollis C. J., Taylor K. W. R., Handley L., Pancost R. D., Huber M., Creech J. B., Hines B. R., Crouch E. M., Morgans H. E. G., Crampton J. S., Gibbs S., Pearson P. N. and Zachos J. C. (2012) Early Paleogene temperature history of the Southwest Pacific Ocean: reconciling proxies and models. *Earth Planet. Sci. Lett.* **349**, 53–66.

Hopmans E. C., Schouten S., Pancost R. D., van der Meer M. T. J. and Sinninghe Damsté J. S. S. (2000) Analysis of intact tetraether lipids in archaeal cell material and sediments by high performance liquid chromatography/atmospheric pressure chemical ionization mass spectrometry. *Rapid Commun. Mass Spectrom.* **14**, 585–589.

Hopmans E. C., Weijers J. W. H., Schefuss E., Herfort L., Sinninghe Damsté J. S. S. and Schouten S. (2004) A novel proxy for terrestrial organic matter in sediments based on branched and isoprenoid tetraether lipids. *Earth Planet. Sci. Lett.* **224**, 107–116.

Huguet C., Hopmans E. C., Febo-Ayala W., Thompson D. H., Sinninghe Damsté J. S. S. and Schouten S. (2006) An improved method to determine the absolute abundance of glycerol dibiphytanyl glycerol tetraether lipids. *Org. Geochem.* **37**, 1036–1041.

Hwang J., Manganini S. J., Montlucon D. B. and Eglinton T. I. (2009) Dynamics of particle export on the Northwest Atlantic margin. *Deep Sea Res. Part I* **56**, 1792–1803.

Ingalls A. E., Shah S. R., Hansman R. L., Aluwihare L. I., Santos G. M., Druffel E. R. M. and Pearson A. (2006) Quantifying archaeal community autotrophy in the mesopelagic ocean using natural radiocarbon. *Proc. Natl. Acad. Sci. U.S.A.* **103**, 6442–6447.

Iverson V., Morris R. M., Frazar C. D., Berthiaume C. T., Morales R. L. and Armbrust E. V. (2012) Untangling genomes from metagenomes: revealing an uncultured class of marine Euryarchaeota. *Science* **335**, 587–590.

Jenkyns H. C., Forster A., Schouten S. and Sinninghe Damsté J. S. S. (2004) High temperatures in the Late Cretaceous Arctic Ocean. *Nature* **432**, 888–892.

Jenkyns H. C., Schouten-Huibers L., Schouten S. and Sinninghe Damsté J. S. S. (2012) Warm Middle Jurassic-Early Cretaceous high-latitude sea-surface temperatures from the Southern Ocean. *Clim. Past* **8**, 215–226.

Karner M. B., DeLong E. F. and Karl D. M. (2001) Archaeal dominance in the mesopelagic zone of the Pacific Ocean. *Nature* **409**, 507–510.

Kim J. H., Schouten S., Buscail R., Ludwig W., Bonnin J., Sinninghe Damste J. S. and Bourrin F. (2006) Origin and distribution of terrestrial organic matter in the NW Mediterranean (Gulf of Lions): application of the newly developed BIT index. *Geochem. Geophys. Geosyst.* **7**. http://dx.doi.org/10.1029/2006GC001306.

Kim J. H., van der Meer J., Schouten S., Helmke P., Willmott V., Sangiorgi F., Koc N., Hopmans E. C. and Sinninghe Damsté J. S. S. (2010) New indices and calibrations derived from the distribution of crenarchaeal isoprenoid tetraether lipids: implications for past sea surface temperature reconstructions. *Geochim. Cosmochim. Acta* **74**, 4639–4654.

Kim J.-H., Villanueva L., Zell C. and Sinninghe Damsté J. S. S. (2016) Biological source and provenance of deep-water derived isoprenoid tetraether lipids along the Portugese continental margin. *Geochim. Cosmochim. Acta* **172**, 177–204.

Kohnen M. E. L., Schouten S., Sinninghe Damsté J. S. S., Deleeuw J. W., Merritt D. A. and Hayes J. M. (1992) Recognition of paleobiochemicals by a combined molecular sulfur and isotope geochemical approach. *Science* **256**, 358–362.

Könneke M., Bernhard A. E., de la Torre J. R., Walker C. B., Waterbury J. B. and Stahl D. A. (2005) Isolation of an autotrophic ammonia-oxidizing marine archaeon. *Nature* **437**, 543–546.

Könneke M., Lipp J. S. and Hinrichs K. U. (2012) Carbon isotope fractionation by the marine ammonia-oxidizing archaeon *Nitrosopumilus maritimus*. *Org. Geochem.* **48**, 21–24.

Könneke M., Schubert D. M., Brown P. C., Hugler M., Standfest S., Schwander T., von Borzyskowski L. S., Erb T. J., Stahl D. A. and Berg I. A. (2014) Ammonia-oxidizing archaea use the most energy-efficient aerobic pathway for CO_2 fixation. *Proc. Natl. Acad. Sci. U.S.A.* **111**, 8239–8244.

Kroopnick P. M. (1985) The distribution of C-13 of $\sum$-CO_2 in the world oceans. *Deep Sea Res. Part A* **32**, 57–84.

Kuypers M. M. M., Blokker P., Erbacher J., Kinkel H., Pancost R. D., Schouten S. and Sinninghe Damsté J. S. S. (2001) Massive expansion of marine archaea during a mid-Cretaceous oceanic anoxic event. *Science* **293**, 92–94.

Laws E. A., Popp B. N., Bidigare R. R., Kennicutt M. C. and Macko S. A. (1995) Dependence of phytoplanktonic carbon isotopic composition on growth rate and $CO_2(aq)$ – Theoretical considerations and experimental results. *Geochim. Cosmochim. Acta* **59**, 1131–1138.

Lin Y. S., Lipp J. S., Elvert M., Holler T. and Hinrichs K. U. (2013) Assessing production of the ubiquitous archaeal diglycosyl tetraether lipids in marine subsurface sediment using intramolecular stable isotope probing. *Environ. Microbiol.* **15**, 1634–1646.

Lincoln S. A., Wai B., Eppley J. M., Church M. J., Summons R. E. and DeLong E. F. (2014) Planktonic Euryarchaeota are a significant source of archaeal tetraether lipids in the ocean. *Proc. Natl. Acad. Sci. U.S.A.* **111**, 9858–9863.

Liu Z., Pagani M. and Zinniker D., et al. (2009) Global cooling during the Eocene-Oligocene climate transition. *Science* **323**, 1187–1190.

Lopes dos Santos R. A., Spooner M. I., Barrows T. T., De Deckker P., Sinninghe Damsté J. S. S. and Schouten S. (2013) Comparison of organic (U-37(K)', TEX_{86}^{H}, LDI) and faunal proxies (foraminiferal assemblages) for reconstruction of late Quaternary sea surface temperature variability from offshore southeastern Australia. *Paleoceanography* **28**, 377–387.

Lourens L. J., Sluijs A., Kroon D., Zachos J. C., Thomas E., Rohl U., Bowles J. and Raffi I. (2005) Astronomical pacing of late Palaeocene to early Eocene global warming events. *Nature* **435**, 1083–1087.

Martens-Habbena W., Berube P. M., Urakawa H., de la Torre J. R. and Stahl D. A. (2009) Ammonia oxidation kinetics determine niche separation of nitrifying Archaea and Bacteria. *Nature* **461**, 976–979.

Massana R., Murray A. E., Preston C. M. and DeLong E. F. (1997) Vertical distribution and phylogenetic characterization of marine planktonic Archaea in the Santa Barbara Channel. *Appl. Environ. Microbiol.* **63**, 50–56.

Mohr W., Tang T., Sattin S. R., Bovee R. J. and Pearson A. (2014) Protein stable isotope fingerprinting: multidimensional protein chromatography coupled to stable isotope-ratio mass spectrometry. *Anal. Chem.* **86**, 8514–8520.

Mollenhauer G. and Eglinton T. I. (2007) Diagenetic and sedimentological controls on the composition of organic matter preserved in California Borderland Basin sediments. *Limnol. Oceanogr.* **52**, 558–576.

Ouverney C. C. and Fuhrman J. A. (2000) Marine planktonic Archaea take up amino acids. *Appl. Environ. Microbiol.* **66**, 4829–4833.

Pancost R. D., Hopmans E. C., Sinninghe Damsté J. S. S. and Party M. S. S. (2001) Archaeal lipids in Mediterranean cold seeps: molecular proxies for anaerobic methane oxidation. *Geochim. Cosmochim. Acta* **65**, 1611–1627.

Pearson A. (1999) *Biogeochemical Applications of Compound-specific Radiocarbon Analysis* Ph.D. Thesis. MIT/WHOI Joint Program, Woods Hole, MA.

Pearson A. (2014) Lipidomics for geochemistry. In *Treatise on Geochemistry*, Vol. 12, Second ed (eds. H. D. Holland and K. K. Turekian), pp. 291–336.

Pearson A. and Eglinton T. I. (2000) The origin of *n*-alkanes in Santa Monica Basin surface sediment: a model based on compound-specific Delta C-14 and delta C-13 data. *Org. Geochem.* **31**, 1103–1116.

Pearson A. and Ingalls A. E. (2013) Assessing the use of archaeal lipids as marine environmental proxies. *Annu. Rev. Earth Planet. Sci.* **41**, 359–384.

Pearson A., McNichol A. P., Benitez-Nelson B. C., Hayes J. M. and Eglinton T. I. (2001) Origins of lipid biomarkers in Santa Monica Basin surface sediment: a case study using compound-specific Delta C-14 analysis. *Geochim. Cosmochim. Acta* **65**, 3123–3137.

Pearson A., Huang Z., Ingalls A. E., Romanek C. S., Wiegel J., Freeman K. H., Smittenberg R. H. and Zhang C. L. (2004) Nonmarine crenarchaeol in Nevada hot springs. *Appl. Environ. Microbiol.* **70**, 5229–5237.

Pester M., Schleper C. and Wagner M. (2011) The Thaumarchaeota: an emerging view of their phylogeny and ecophysiology. *Curr. Opin. Microbiol.* **14**, 300–306.

Pitcher A., Wuchter C., Siedenberg K., Schouten S. and Sinninghe Damsté J. S. S. (2011) Crenarchaeol tracks winter blooms of ammonia-oxidizing Thaumarchaeota in the coastal North Sea. *Limnol. Oceanogr.* **56**, 2308–2318.

Prahl F. G., Hayes J. M. and Xie T. M. (1992) Diploptene – An indicator of terrigenous organic carbon in Washington coastal sediments. *Limnol. Oceanogr.* **37**, 1290–1300.

Prahl F. G., Ertel J. R., Goni M. A., Sparrow M. A. and Eversmeyer B. (1994) Terrestrial organic carbon contributions to sediments on the Washington Margin. *Geochim. Cosmochim. Acta* **58**, 3035–3048.

Qin W., Amin S. A., Martens-Habbena W., Walker C. B., Urakawa H., Devol A. H., Ingalls A. E., Moffett J. W., Armbrust E. V. and Stahl D. A. (2014) Marine ammonia-oxidizing archaeal isolates display obligate mixotrophy and wide ecotypic variation. *Proc. Natl. Acad. Sci. U.S.A.* **111**, 12504–12509.

Qin W., Carlson L. T., Armbrust E. V., Devol A. H., Moffett J. W., Stahl D. A. and Ingalls A. E. (2015) Confounding effects of oxygen and temperature on the TEX_{86} signature of marine Thaumarchaeota. *Proc. Natl. Acad. Sci. U.S.A.* **112**, 10979–10984.

Saenz J. P., Wakeham S. G., Eglinton T. I. and Summons R. E. (2011) Abundance and structural diversity of bacteriohopanepolyols in suspended particulate matter along a river to ocean transect. *Org. Geochem.* **42**, 774–780.

Santoro A. E. and Casciotti K. L. (2011) Enrichment and characterization of ammonia-oxidizing archaea from the open ocean: phylogeny, physiology and stable isotope fractionation. *ISME J.* **5**, 1796–1808.

Santoro A. E., Casciotti K. L. and Francis C. A. (2010) Activity, abundance and diversity of nitrifying archaea and bacteria in the central California Current. *Environ. Microbiol.* **12**, 1989–2006.

Santoro A. E., Dupont C. L., Richter R. A., Craig M. T., Carini P., McIlvin M. R., Yang Y., Orsi W. D., Moran D. M. and Saito M. A. (2015) Genomic and proteomic characterization of "*Candidatus* Nitrosopelagicus brevis": an ammonia-oxidizing archaeon from the open ocean. *Proc. Natl. Acad. Sci. U.S.A.* **112**, 1173–1178.

Schmittner A., Gruber N., Mix A. C., Key R. M., Tagliabue A. and Westberry T. K. (2013) Biology and air-sea gas exchange controls on the distribution of carbon isotope ratios (delta C-13) in the ocean. *Biogeosciences* **10**, 5793–5816.

Schouten S. (1995) *Structural and Stable Carbon Isotope Studies of Lipids in Immature Sulphur-rich Sediments* Ph.D. Thesis. University of Groningen, The Netherlands, pp. 306.

Schouten S., Hoefs M. J. L., Koopmans M. P., Bosch H. J. and Sinninghe Damsté J. S. S. (1998) Structural characterization, occurrence and fate of archaeal ether-bound acyclic and cyclic biphytanes and corresponding diols in sediments. *Org. Geochem.* **29**, 1305–1319.

Schouten S., Wakeham S. G. and Sinninghe Damsté J. S. S. (2001) Evidence for anaerobic methane oxidation by archaea in euxinic waters of the Black Sea. *Org. Geochem.* **32**, 1277–1281.

Schouten S., Hopmans E. C., Schefuss E. and Sinninghe Damsté J. S. S. (2002) Distributional variations in marine crenarchaeotal membrane lipids: a new tool for reconstructing ancient sea water temperatures? *Earth Planet. Sci. Lett.* **204**, 265–274.

Schouten S., Pitcher A., Hopmans E. C., Villanueva L., van Bleijswijk J. and Sinninghe Damsté J. S. S. (2012) Intact polar and core glycerol dibiphytanyl glycerol tetraether lipids in the Arabian Sea oxygen minimum zone: I. Selective preservation and degradation in the water column and consequences for the TEX86. *Geochim. Cosmochim. Acta* **98**, 228–243.

Schouten S., Hopmans E. C. and Sinninghe Damsté J. S. S. (2013) The Org. Geochem. of glycerol dialkyl glycerol tetraether lipids: a review. *Org. Geochem.* **54**, 19–61.

Schubotz F., Lipp J. S., Elvert M. and Hinrichs K. U. (2011) Stable carbon isotopic compositions of intact polar lipids reveal complex carbon flow patterns among hydrocarbon degrading microbial communities at the Chapopote asphalt volcano. *Geochim. Cosmochim. Acta* **75**, 4399–4415.

Sessions A. L., Sylva S. P. and Hayes J. M. (2005) Moving-wire device for carbon isotopic analyses of nanogram quantities of nonvolatille organic carbon. *Anal. Chem.* **77**, 6519–6527.

Shah S. R. and Pearson A. (2007) Ultra-microscale (5–25 mu g C) analysis of individual lipids by C-14 AMS: assessment and correction for sample processing blanks. *Radiocarbon* **49**, 69–82.

Shah S. R., Mollenhauer G., Ohkouchi N., Eglinton T. I. and Pearson A. (2008) Origins of archaeal tetraether lipids in sediments: insights from radiocarbon analysis. *Geochim. Cosmochim. Acta* **72**, 4577–4594.

Sinninghe Damsté J. S. S., Ossebaar J., Abbas B., Schouten S. and Verschuren D. (2009) Fluxes and distribution of tetraether lipids in an equatorial African lake: constraints on the application of the TEX_{86} palaeothermometer and BIT index in lacustrine settings. *Geochim. Cosmochim. Acta* **73**, 4232–4249.

Smittenberg R. H., Baas M., Green M. J., Hopmans E. C., Schouten S. and Sinninghe Damsté J. S. S. (2005) Pre- and post-industrial environmental changes as revealed by the biogeochemical sedimentary record of Drammensfjord, Norway. *Mar. Geol.* **214**, 177–200.

Spang A., Hatzenpichler R., Brochier-Armanet C., Rattei T., Tischler P., Spieck E., Streit W., Stahl D. A., Wagner M. and Schleper C. (2010) Distinct gene set in two different lineages of ammonia-oxidizing archaea supports the phylum Thaumarchaeota. *Trends Microbiol.* **18**, 331–340.

Stadnitskaia A., Ivanov M. K. and Sinninghe Damsté J. S. S. (2008) Application of lipid biomarkers to detect sources of organic matter in mud volcano deposits and post-eruptional methanotrophic processes in the Gulf of Cadiz, NE Atlantic. *Mar. Geol.* **255**, 1–14.

Stieglmeier M., Klingl A., Alves R. J. E., Rittmann S. K. M. R., Melcher M., Leisch N. and Schleper C. (2014) Nitrososphaera viennensis gen. nov., sp nov., an aerobic and mesophilic, ammonia-oxidizing archaeon from soil and a member of the archaeal phylum Thaumarchaeota. *Int. J. Syst. Evol. Microbiol.* **64**, 2738–2752.

Swart P. K., Greer L., Rosenheim B. E., Moses C. S., Waite A. J., Winter A., Dodge R. E. and Helmle K. (2010) The ^{13}C Suess effect in scleractinian corals mirror changes in the anthropogenic CO_2 inventory of the surface oceans. *Geophys. Res. Lett.* **37**, L05604.

Tan F. C. and Strain P. M. (1979) Organic carbon isotope ratios in recent sediments in the St. Lawrence estuary and the Gulf of St. Lawrence. *Estuarine Coastal Mar. Sci.* **8**, 213–225.

Tan F. C. and Strain P. M. (1983) Sources, sinks and distribution of organic carbon in the St. Lawrence estuary, Canada. *Geochim. Cosmochim. Acta* **47**, 125–132.

Taylor K. W. R., Huber M., Hollis C. J., Hernandez-Sanchez M. T. and Pancost R. D. (2013) Re-evaluating modern and Palaeogene GDGT distributions: implications for SST reconstructions. *Global Planet. Change* **108**, 158–174.

Thomas C. J., Blair N. E., Alperin M. J., DeMaster D. J., Jahnke R. A., Martens C. S. and Mayer L. (2002) Organic carbon deposition on the North Carolina continental slope off Cape Hattaras (USA). *Deep Sea Res. Part II* **49**, 4687–4709.

Tierney J. E. and Tingley M. P. (2014) A Bayesian, spatially-varying calibration model for the TEX_{86} proxy. *Geochim. Cosmochim. Acta* **127**, 83–106.

Tierney J. E. and Tingley M. P. (2015) A TEX_{86} surface sediment database and extended Bayesian calibration. *Nat. Sci. Data* **2**, 150029–150029.

Tierney J. E., Mayes M. T., Meyer N., Johnson C., Swarzenski P. W., Cohen A. S. and Russell J. M. (2010) Late-twentieth-century warming in Lake Tanganyika unprecedented since AD 500. *Nat. Geosci.* **3**, 422–425.

Tourna M., Stieglmeier M., Spang A., Könneke M., Schintlmeister A., Urich T., Engel M., Schloter M., Wagner M., Richter A. and Schleper C. (2011) *Nitrososphaera viennensis*, an ammonia oxidizing archaeon from soil. *Proc. Natl. Acad. Sci. U.S.A.* **108**, 8420–8425.

Turich C., Freeman K. H., Bruns M. A., Conte M., Jones A. D. and Wakeham S. G. (2007) Lipids of marine Archaea: patterns and provenance in the water-column and sediments. *Geochim. Cosmochim. Acta* **71**, 3272–3291.

Wakeham S. G., Lewis C. M., Hopmans E. C., Schouten S. and Sinninghe Damsté J. S. S. (2003) Archaea mediate anaerobic oxidation of methane in deep euxinic waters of the Black Sea. *Geochim. Cosmochim. Acta* **67**, 1359–1374.

Walker C. B., de la Torre J. R., Klotz M. G., Urakawa H., Pinel N., Arp D. J., Brochier-Armanet C., Chain P. S. G., Chan P. P., Gollabgir A., Hemp J., Hugler M., Karr E. A., Könneke M., Shin M., Lawton T. J., Lowe T., Martens-Habbena W., Sayavedra-Soto L. A., Lang D., Sievert S. M., Rosenzweig A. C., Manning G. and Stahl D. A. (2010) *Nitrosopumilus maritimus* genome reveals unique mechanisms for nitrification and autotrophy in globally distributed marine crenarchaea. *Proc. Natl. Acad. Sci. U.S.A.* **107**, 8818–8823.

Walsh J. J., Premuzic E. T., Gaffney J. S., Rowe G. T., Harbottle G., Stoenner R. W., Balsam W. L., Betzer P. R. and Macko S. A. (1985) Organic storage of CO_2 on the continental slope off the Mid-Atlantic Bight, the Southeastern Bering Sea, and the Peru Coast. *Deep Sea Res. Part II* **32**, 853–883.

Walsh E. M., Ingalls A. E. and Keil R. G. (2008) Sources and transport of terrestrial organic matter in Vancouver Island fjords and the Vancouver-Washington Margin: a multiproxy approach using delta C-13(org), lignin phenols, and the ether lipid BIT index. *Limnol. Oceanogr.* **53**, 1054–1063.

Weijers J. W. H., Schouten S., Hopmans E. C., Geenevasen J. A. J., David O. R. P., Coleman J. M., Pancost R. D. and Sinninghe Damsté J. S. S. (2006) Membrane lipids of mesophilic anaerobic bacteria thriving in peats have typical archaeal traits. *Environ. Microbiol.* **8**, 648–657.

Wuchter C., Schouten S., Boschker H. T. S. and Sinninghe Damsté J. S. S. (2003) Bicarbonate uptake by marine Crenarchaeota. *FEMS Microbiol. Lett.* **219**, 203–207.

Wuchter C., Abbas B., Coolen M. J. L., Herfort L., van Bleijswijk J., Timmers P., Strous M., Teira E., Herndl G. J., Middelburg J. J., Schouten S. and Sinninghe Damsté J. S. S. (2006) Archaeal nitrification in the ocean. *Proc. Natl. Acad. Sci. U.S.A.* **103**, 12317–12322.

Xie S. T., Liu X. L., Schubotz F., Wakeham S. G. and Hinrichs K. U. (2014) Distribution of glycerol ether lipids in the oxygen minimum zone of the Eastern Tropical North Pacific Ocean. *Org. Geochem.* **71**, 60–71.

Yerkes R. F., McCulloh T. H., Schoellhamer J. E. and Vedder J. G. (1965) Geology of the Los Angeles Basin California – An introduction. *U.S. Geol. Surv., Prof. Pap.* **420-a**, 64.

Associate editor: Elizabeth Ann Canuel